2012

The Applications of Enriched Finite Element Analysis in Electronic Packaging

Yi Chen
Lehigh University

THE APPLICATIONS OF ENRICHED FINITE ELEMENT ANALYSIS IN ELECTRONIC PACKAGING

by
Yi Chen

A Thesis
Presented to the Graduate and Research Committee
of Lehigh University
in Candidacy for the Degree of
Master of Science

in
Mechanical Engineering and Mechanics

Lehigh University
May 2012

This thesis is accepted and approved in partial fulfillment of the requirements for the Master of Science

_____

Date

_____

Thesis Advisor

_____

Chairperson of Department

Acknowledgements

I would like to extend my deepest gratitude to my advisor, Professor Herman F. Nied at Lehigh University, the department of Mechanical Engineering and Mechanics. I have been known with Professor Nied I came to Lehigh, he is always a very nice and admirable scholar, and is very popular among students. Not only because his friendliness and humorous, but also his academic talent and great engineering knowhow as well!

Also, I want to express my sincere thanks to all the lab mates that I have been worked with. PhD candidate Xiao Liu and I have been worked in the same project for 2 years, and he is always within help whenever I have difficulties on my research work. PhD candidate Pornsak Thasanaraphan is a very diligent scholar from Thailand, and he is very positive to life and always encourages me for my future career and life. PhD candidate Johann Pancrace and his wife Nguyen Nenuphar are very good friend of mine, and we had very good time together for 1 year together. I also want to thank my other lab mates Bon Seung Koo, Guosong Zeng, Jeremy Payne and Bora Baloglu for their friendliness and other help for me.

Finally, I want to thank my parents, Aizhen Chen and Hongxiang Wang, for their supports, hope and braveness they bring to me all the way from our home in Shanghai, China. My fiancée, Haoyong Sun is a very smart and graceful girl, who is my greatest support here in the USA.

Table of Contents

Acknowledgements iii
1 Introduction and Background 3
1.1 Electronic Packaging 3
1.2 Problem with Packaging 4
1.3 Fracture Mechanics Theory 5
1.4 Finite Element Analysis 7
1.5 State of Arts 8
1.5.1 Experiment Based Techniques 9
1.5.2 Computation Based Simulations 9
1.6 Objective 10
2 Compile and Link the UDE 12
2.1 Introduction to UDE 12
2.2 Compile the UDE 14
2.3 Link the UDE 15
2.4 Comparison of FRAC3D and USER300 17
3 Computation 19
3.1 Review of Fatigue Crack Growth Propagation 19
3.1.1 Stages of Fatigue Crack Growth 19
3.1.2 Classic Models for Fatigue Crack Propagation 22
3.1.3 System-Level Packaging Thermal Management and Optimization 24
3.2 3D Modeling of Interface Crack in ANSYS 25
3.2.1 Geometry and Load 25
3.2.2 Material Property and Fatigue Algorithm 27
3.2.3 Apply Enriched UDE 28
3.3 3D Modeling of System-Level Package 31
3.3.1 Processing and Flow Chart 31
3.3.2 Configuration of the System 31
3.3.3 Optimized Configuration of the System 35
4 Result and Conclusion 37

4.1 Crack Problem Solution 37
4.2 Thermal Management Solution 39
4.2.1 Case #1 Fan mount on chip 39
4.2.2 Case #2 Fan mount on body with heat sink on chip 41
4.3 Conclusion 45
5 Future Work 46
6 List of Abbreviations and Symbols 49
Reference 50

Table of Figures

Figure 1 Independent modes of crack deformation [5] 6
Figure 2 A series of C-SAM images of the progression of a corner crack at the interface 11
Figure 3 ANSYS Product Launcher to run the customized ANSYS executable 13
Figure 4 "*Customization/Preference*" Tab in ANSYS Launcher 13
Figure 5 Copy and substitute the UDE_f3d.lib and UserElem.F from successfully compiled desktops 16
Figure 6 Use ANSYSCUST.BAT to create a User Defined "ansys.exe" 16
Figure 7 Comparison of the flow charts of calculation procedure 17
Figure 8 Stages of the Crack Propagation 19
Figure 9 Fatigue Striations in Stainless Steel (Courtesy C.D. Beachem, P.E.) 21
Figure 10 Circular cracks in an infinite solid as a special case of an elliptical crack 25
Figure 11 ¼ model of Silicon/BCB interfacial crack propagation under thermal loading 26
Figure 12 Advance of the crack front nodes in crack growth algorithm method. 28
Figure 13 User Defined Elements (USER300) along the crack front 29
Figure 14 Multi-dialog indicating the basic information of the computing 30
Figure 15 Flow chart of conducting simulation in ANSYS Workbench 31
Figure 16 Solid model of the electronic system in Pro Engineer 33
Figure 17 (a) Solid model of the electronic system #1 in IcePak (b) Meshing of the Electronic system #1 34
Figure 18 (a) Solid model of the electronic system #2 (b) Meshing of the electronic system #2 36
Figure 19 Interfacial crack propagation of the bi-material under thermal loading 38
Figure 20 First stress intensity factor, K I along the crack front 39
Figure 21 Temperature distribution of the electronic system #1 40
Figure 22 Temperature distribution of the PCB board in system #1 40
Figure 23 Airflow speed contour in the system configuration #1 41
Figure 24 Temperature distribution in the system #1 42
Figure 25 Temperature distribution of the PCB board in system #2 43
Figure 26 Airflow speed contour of the system configuration #2 44
Figure 27 Flow chart for the feasibility of joint work of IcePak and APDL 47
Figure 28 Different modules for the multi-physics simulation in WorkBench 48

Abstract

The electronic packaging is one of the key technologies that determine the reliability and durability of electronic devices. As the electronic devices have better mobility, become smaller in size and have higher performance, the electronic packaging is required to provide even better protection.

Fracture mechanics has been a traditional subject back to the World War I. It was originated by a British aeronautical engineer, Alan A. Griffith. He suggested that the lower fracture strength observed in experiments than its theoretical value, together with the size-dependence of strength, was due to the presence of microscopic flaws in the material [1]. Since then, fracture mechanics theory has been applied to broader areas: pressure vessel, aerospace and aeronautics, metal, ceramic and composite materials. One recent advance of the fracture mechanics theory is being used in the electronic packaging industry. Since the current electronic packaging requires the connection of material with distinct material properties, thermal expansion difference induced fracture will cause the physical failure of the electronics.

In this study, enriched finite element was extracted from the FRAC3D solver, and was seamlessly transferred into the user defined element, USER300, in software ANSYS. An example of fatigue crack propagation was then exhibited to predict the crack growth by classic Paris-Erdogan law with USER 300 element.

Some new advances of the finite element analysis for electronic packaging were presented. IcePak is very user-friendly finite element analysis software that was released by ANSYS recently. It integrates multi-physics analysis specific for electronic packaging. For example, IcePak contains a library of pre-defined fan, chip package, heat source that are ready for analysis.

Once the setup is done, IcePak provides sophisticated answers of airflow analysis, thermal exchange analysis, and mechanical property analysis as well.

Finally, an additional feature of the ANSYS is it has a brand new way of doing engineering analysis called WorkBench. The WorkBench provides user with a framework that contains different modules in it. With WorkBench, the classic APDL, IcePak or Fluent are different modules. They can be combined together, and use the result from one module as the input for the other module. In the following discussion, one example of optimizing the heat dissipation of an electronic system will be presented. Also, the feasibility of combining the user defined finite element for fracture analysis and thermal analysis with IcePak will be discussed.

1 Introduction and Background

1.1 Electronic Packaging

The electronic packaging technologies are a whole range of design, analysis, micro-manufacturing, and some unique processing for thin film, vacuum, sheet metal and semiconductor approaches. Now, two major soldering technologies are commonly employed for the mass production of semiconductor packaging: plate-through-hole (PTH) and surface mount technology (SMT).

Plate-through-hole is the use of leads on electronic components and inserting them into the holes drilled on the Printed Circuit Boards (PCBs). The leads are then soldered on the opposite side of the PCB board. While PTH technology provides strong mechanical bonds for the electronics, the additional drilling limits it application, because it is more expensive to produce and limits the available routing area for signal traces.

In recent years, surface mount technology plays a key role in various levels of electronic packaging. It is the use of solder joints to serve critical electrical and mechanical connection for the chip to be mounted on the PCBs, such as flip-chip connection, solder-ball connection in ball-grid-arrays (BGA), and IC packaging.

The fundamental difference between PTH and SMT is their interconnection scheme. In PTH, solder joints are utilized in the plated-through-holes on a PCB. The molten solder is directly applied to the area of PTH and fills the gap between I/O pin and the plate by capillary force. SMT is more commonly used in today's electronic packaging industry, where I/O leads are pre-attached to the PCB surface. The advantage of SMT is it eliminates most penetrated holes in the PCB by utilizing both surfaces of PCB to place components [2]. Also, SMT have a finer lead

pitch and smaller package size, which allows higher packaging density than the traditional plated-through-holes technology.

1.2 Problem with Packaging

Usually, there is no single factor that causes the failure or malfunction of the electronic parts. The failure mode of electronic components has various causes: it can be caused by excess temperature that overheat the electronic device, excess current or voltage that shock the circuit, ionizing radiation, mechanical sock, stress or impact that cause the physical failure. As a matter of fact, however, most of the electronic components failure are packaging related. This is because the packaging provides a "bridge" between the electronics and the outside environment. During service, the electronic packaging is under various environments. Failures caused by excess temperature, current or voltage, ionizing radiation, mechanical shock, stress or impact and many other circumstances can always initiate from the packaging.

Scholars and researchers from both academia and industry worldwide have spent years of efforts in unveiling the mechanism and predicting the failure. B. Su, Y.C. Lee and M. Dunn [3] studied a class of solder bumps with different size and shape, jointed on a brittle GaAs die and are subjected to a uniform temperature change. They reported that the crack of the solder bump is directly related to temperature and the size of the bump, smaller bumps require larger temperature change to induce cracking. S.B. Lee, I. Kim and T.S. Park [4] utilized small size electromagnetic bending cycling tester, micro mechanical testing machine, and other thermal fatigue testing apparatus to assess the failure mechanisms of electronics packaging. They also compared the fatigue with pure mechanical load to the thermal fatigue. It was concluded that the thermal loading fatigue has a shorter life than the mechanical load at same inelastic energy dissipation cycle.

Among all different factors that cause electronic failure, thermal expansion mismatch between materials that produces high interfacial mechanical stresses is one of the most important factors. The packaging underfill material has much higher thermal expansion coefficient, compared to the electronics material. Thermal expansion mismatch causes interface delamination between the epoxy molding compound, silicon die as well as the copper leadframe interface.

In addition, initial micro cracks that are inevitable during manufacturing process will easily propagate through the interface due to the thermal expansion mismatch of the packaging materials, and destroy the electronic device by cutting off its connection. Thus, stronger and more reliable packaging is needed to protect the electronic components.

1.3 Fracture Mechanics Theory

Fracture mechanics has been a very important subject in engineering mechanics since the World War I, here the study is mainly focused on the crack propagation of fracture mechanics. It is reported that fatigue crack growth exists in over 80% of all brittle fractures. From a safety point of view, the real danger of fatigue crack growth is its hidden nature. The failures caused by fatigue crack growth occur suddenly and usually without obvious precursors to warn the sudden failure. This is dramatically different from other structures under over-loading, that the deflection become larger or deformation retain after the removal of load, and is obvious. Therefore, any structure should be expected to have free surfaces, and may eventually experience fatigue crack growth and grow to reach critical dimension for brittle failure. Thus, regular check and careful maintenance, or good prediction of the fatigue crack propagation is extremely important to the prevention of fracture failure.

One common problem of fracture is a line discontinuity that represents the crack in the solid geometry, which ends abruptly with a zero radius cut. As a consequence of this type of problem, the stresses at the tip of the crack tend to be infinity. Nevertheless, the resulting infinite stresses seem to be inconsistent with the finite applied loads in our real world. In fact, regardless of the geometry or different types of loading, all singular crack tip problems in elastic bodies share commonly the distribution of stress, strain and displacement over the surrounding crack tip region.

The difference of deformation fields produced by symmetric or antisymmetric results in the different motions of the crack faces, namely: Opening Mode, Forward Mode and Shear Mode, shown in Figure 1. Mode I loading occurs for cracks under tensile loading; Mode II, represents sliding or shearing of the material; Mode III, is a tearing shear of the material.

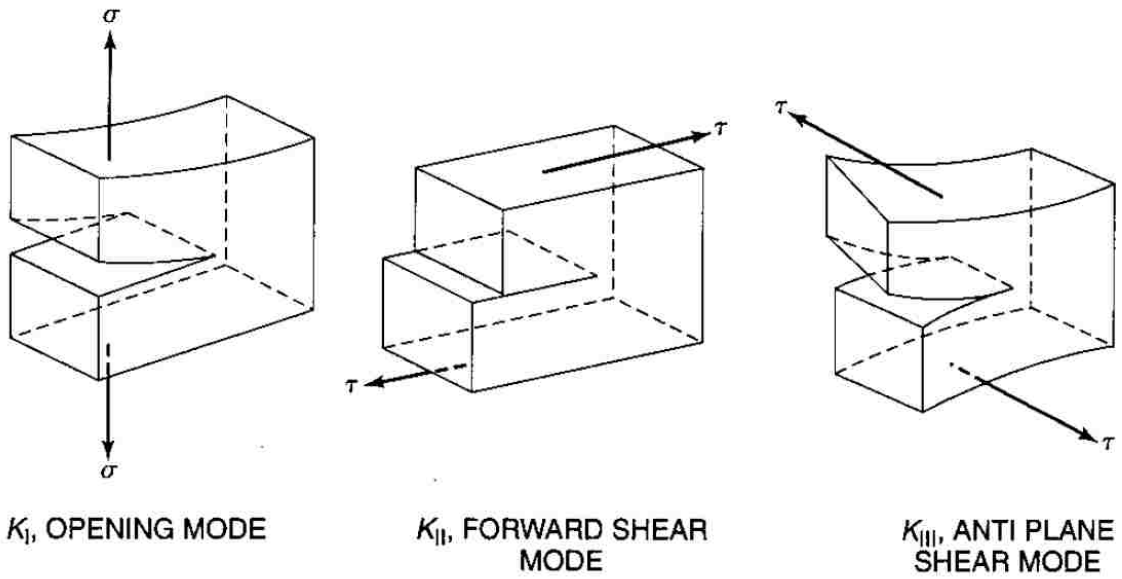

Figure 1 Independent modes of crack deformation [5]

1.4 Finite Element Analysis

In 1943 R. Courant [6], first developed the Finite Element Analysis (FEA) method and its fundamental theories, where he used the Ritz method of numerical mathematics and variational calculus to solve vibration systems. Since then, the finite element theories have attracted many of the engineers in industry, as well as researchers from academia. M. J. Turner, R. W. Clough, H. C. Martin and L. J. Topp have published a series of paper on the FEA method. However, since the numerical calculation methods was mostly limited to human works and large-scale matrix transformation and solution were tedious and almost impossible to be done with hand calculation, the advantage of finite element method was very limited.

Development of the FEA method began in the middle of 1950, where John Argyris and Ray, Clough started to gather momentum for the design of airframe and some basic structural analysis [7]. By early 1970's, the FEA method was still exclusively employed by the aeronautics, automotive, defence, and nuclear industries. Though modern computers are already available at that time, the cost of mainframe computer was still very expensive. Also, due to the relatively low performance of those computers, FEA can only be applied in simple structure analysis, without much complicated geometry and have many details in it.

Since the decline of the cost of microcomputers, the FEA has become commonplace in recent years, and now occupies multibillion dollars per year in industry. Numerical problems of very complicated stress problems can now be solved easily by using FEA [8]. Besides, due to the fast speed of the workstations, modern FEA software and in-house codes are able to solve much more complicated engineering problems with multi-physics fields in very short time.

In this paper, this part of research is mainly done with in commercial available FEA software, ANSYS, developed by ANSYS Corporation in Canonsburg, Pennsylvania. Also, a specialized code, FRAC3D with enriched finite element specific for the calculation of fracture mechanics was developed here at Lehigh University, and will be integrated into the ANSYS through a user defined feature, namely the "USER300". Detailed information will be discussed in the following parts. There will also be an example of fatigue crack propagation done in FRAC3D from the previous studies, and it will now be done in ANSYS.

Beside classic ANSYS, ANSYS Workbench is a framework which is now widely used in industry and academia. With the release of ANSYS 12 in 2009, the Workbench framework has been changed significantly. It offers a comprehensive multi-physics solution within a single platform which includes: structural, thermal, fluid and electromagnetic analysis, and combines the advantage of different ANSYS solver with the project management tools to manage the project workflow [9]. In the Workbench, analysis is built into each module, which can be combined into a whole project. The project is then driven by a schematic workflow that manipulates the connections between different modules.

1.5 State of Arts

From material strength point of view, predefined critical loads or average stresses are commonly used to assess the strength of material interface. However, even if the stresses are far below the material yield strength, crack in the bi-material interface will still propagate under fatigue cycling. One way to quantify the critical crack propagation force is to measure the ultimate strength that the bi-material interface can sustain before interface crack move during the tensile or shear testing.

1.5.1 Experiment Based Techniques

Experiment-based testing for the fracture toughness has been widely done by the researchers worldwide, to characterize the material properties. Th. Seeling, Gross, and K. Pothmann [10] used special numerical method to investigate the time history of mode I and mode II stress intensity factors for the compact compression specimens, and discussed aspects of model setup as well as the boundary element method. They applied precracked compression specimens for testing the dynamic crack propagation, and experimentally got the dynamic fracture toughness for the material property for the numerical calculation. Horacio D. Espinosa and Bei Peng [11] developed a new membrane deflection fracture experiment, and investigated the fracture toughness of the MEMS system and other thin film materials. They preformed a 100 nm radius notch in the material and concluded that the fracture toughness is independent of crack length. Charles, Veronique and etc [12] proposed a micromechanical model to describe the interconnection between the microstructure and deformation mechanisms in ferritic steels under cyclic loading. They tried to improve the material fatigue property through optimize the microstructure of steels.

1.5.2 Computation Based Simulations

Fan, Chung and etc., [13] conducted a series of button shear test to evaluate the bi-material adhesion properties with different preconditions, where a critical strain energy density was tested for the initiation of delamination at epoxy molding compound/copper leadframe interface.

Among all different strength-based crack prediction approaches, strain energy density based theory is a very common criterion, which assumes the crack failure occurs where the strain energy density exceeds a critical value. Andrew A.O. and T.Y. Lin [14] measured the interfacial fracture toughness as a function of temperature and relative humidity. They found that whether

the edge crack will propagate depends on the ratio of the mode II interface toughness to that of mode I interface toughness. R. Khandelwal and J.M. Chandra Kishen [15] analyzed the Stress Intensity Factors, SIFs in a linear bi-material elastic body containing a crack at the interface and subjected to thermal loading. A.F. Herr and H.F. Nied [16] used the enriched finite elements in FRAC3D for the simulation of crack propagation with circular or penny-shaped initial cracks. They found that the final shape of the crack has no relation to the initial shape of the crack. Though satisfied results can be achieved, the original program involves separate codes developed at Lehigh University MEMS Department, so that using these codes needs the study on additional materials. Ayhan [17] created a user guide with detailed explanation and examples for this procedure. However, the program is still not convenient for extensive application in industry. Besides, this process requires much manual work by the users, including importing nodal coordinates, connectivity, loads and B.C.s from ANSYS, inputting parameters to generate the geometry file (.geo), the controlling file (.run) for FRAC3D, and setting up to run the analyzer.

1.6 Objective

The objective of this study is to use fracture mechanics theory with Finite Element Analysis (FEA) method to predict the 3D interface fatigue crack propagation in semiconductor packaging. An experimental result of C-SAM from Sandia National Lab was shown in Figure 2, where the fatigue thermal crack propagation is presented. A Customized finite element, USER 300, in commercial available FEA software ANSYS will be compiled with the Enriched Finite Element Analysis developed at Lehigh University, and will simulate the fatigue crack growth similar to this experimental result.

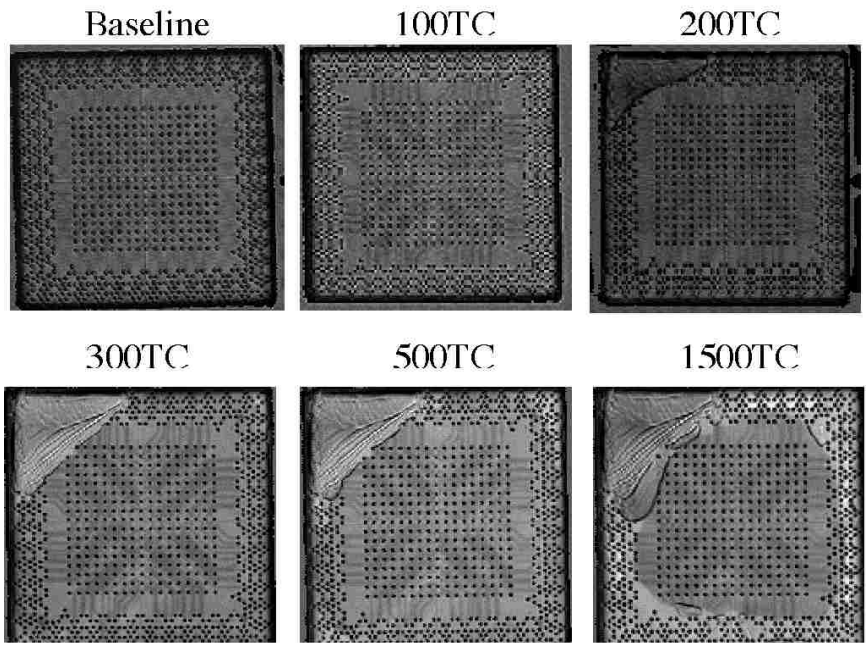

Figure 2 A series of C-SAM images of the progression of a corner crack at the interface

Two commonly used loading scenarios, pure mechanical loading and thermal mechanical loading will be analyzed on the chip-level packaging. The model is assumed to be existed a precrack in the bi-material interface, and the crack growth trend will be predicted with a classic crack propagation law, Paris-Erdogan law. Also, some new applications of the ANSYS Workbench and IcePak will be shown on a system-level packaging. The simulation of fluid flow and cooling circulation inside an electronic system will be presented. The electronic system is a desktop workstation which has two different configurations with independent heat management solution. Their advantage and efficiency of dissipating heat will be discussed. Finally, one future development of combining USER 300 enriched finite element and IcePak or Workbench will be discussed in the last part.

2 Compile and Link the UDE

2.1 Introduction to UDE

User Programmable Features (UPFs) are ANSYS capabilities that allow the user to write their own routines, and tailor the ANSYS program to specific needs. For instance, the users might want to define a new material behavior, a modified element, or a special failure criterion for composite materials [18].

In this section, a customized finite element in ANSYS, USER 300 is incorporated into the Enriched Finite Element (UDE), which was mentioned in the first section. It is used to substitute the original way of calculate the fracture mechanics, called FRAC3D, which is a specialized code developed at Lehigh University for fracture mechanics calculation. The new USER 300 element is one of the customizable features of the UDFs in ANSYS, and is used to simulate the fatigue crack propagation by taking the Stress Intensity Factors (SIFs) as additional Degree of Freedom (DOF).

ANSYS 12.1 is recompiled for the new features of calculating the SIFs using FORTRAN compiler. Several necessary files are copied from ANSYS default folder and modified, and the users can then add their own subroutines, library files or other relative files into the compiling and linking folder.

After the compile is done, a custom executable “ANSYS.exe” is then generated, Figure 3, and it can be launched in the ANSYS Mechanical APDL Product Launcher with Customization/Preference, Figure 4. This special executable contains all important features transferred from the in-house code FRAC3D. Now it is ready to perform the user-defined computation for fracture mechanics. The brief description of compiling and linking the software

will be discussed here, and step-by-step guide for how this process is performed can be found in Yi and Xiao's [19] User Guide of the User-Defined Enriched Finite Element in ANSYS.

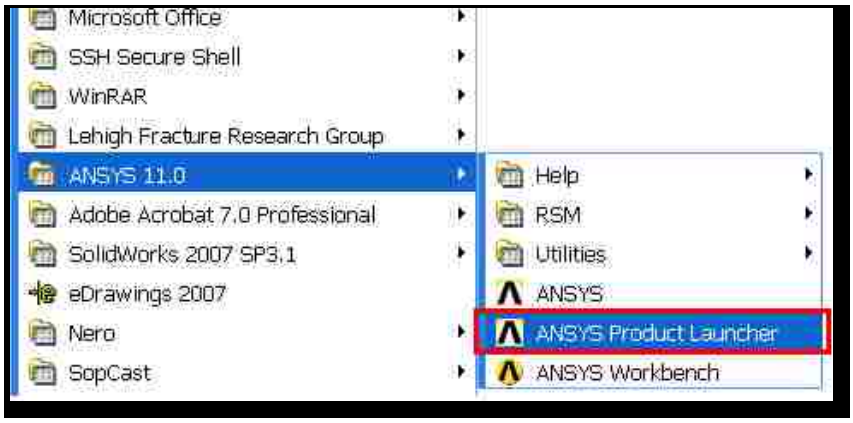

Figure 3 ANSYS Product Launcher to run the customized ANSYS executable

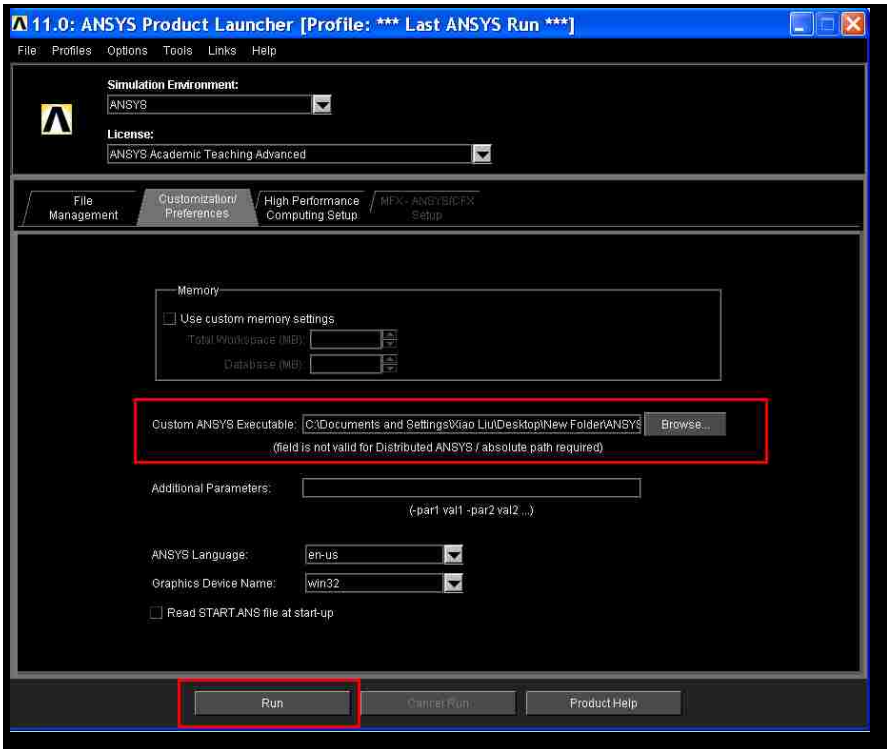

Figure 4 "*Customization/Preference*" Tab in ANSYS Launcher

2.2 Compile the UDE

For the ANSYS 12.1 Student Edition used in this study, following software has been employed to compile the UDE:

- ✓ Development Platform: Microsoft Visual Studio 2005 IDE
- ✓ C++ Compiler: Microsoft Visual C++ 2005
- ✓ FORTRAN Compiler: Intel Fortran Compiler 10.1.021

Microsoft Visual Studio 2005 has been verified to be working on both version 11.0 and 12.1 of ANSYS. It is anticipated to use the latest version of these compilers, but other equivalent compilers should also work. Typically, the FORTRAN compiler is installed after the Microsoft compiler, and is updated to include the path of Microsoft linker.

A general overview of compiling the UPFs would be as follows:

- Set up an appropriate development environment
- Find the useful subroutines and related files in the "custom" or "customized" directory and put them into the working directory
- Modify the subroutines accordingly
- With the supported compiler, compile subroutines to create the object file
- With the supported linker, link the compiled object file and supplied libraries to create a customized ANSYS executable

Typically, the Microsoft compiler is installed prior to the FORTRAN compiler. Then the FORTRAN compiler is updated to account the path to Microsoft linker, which provides the compiling path. After the installation of both compilers completed, a batch file called "IFORTVARS.BAT" should be then replaced with a call to the appropriate Microsoft Visual

Studio batch file. After that, the "IFORTVARS.BAT" batch can be called to set up the correct PATH, LIB and INCLUDE variables for the FORTRAN compiler and Microsoft linker. Users were then required to specify the full path of the batch file in "ANCUST.BAT" under "custom/user" folder. Other necessary files from ANSYS are ANSCUST.BAT, anasyslarge.def, anasyssmall.def, as well as the MAKEFILE. These files are located in the ANSYS's "custom folder", which contains all the user-defined subroutines.

After this step, the compiling work is almost done, it usually take a while for the system to finish the compiling work in its original folder. However, users can copy the necessary files mentioned above to another directory and do the compiling work in a newly specified folder. There is no restriction of the location that users define their working directory for this compiling and linking work.

2.3 Link the UDE

In the previous section 2.2, ANSYS was recompiled with FORTRAN compiler for the UDE, but this requires a specific version of platform and compiler, as well as experienced programmer to modify the subroutine and work on the compilation.

For additional convenience, an alternative way of generating the customized ANSYS executable is simply use the successfully compiled files, which in this case is a library file called "UDE_f3d.lib". Should the enriched finite element or USER300 feature be used in larger lab with hundreds of workstations, once the compile is done on one of them, other workstations can be simply "linked", and generate the executable. The users just need to compile the subroutine "UserElem.F", together with the modules subroutine "allmodules.f90" from FRAC3D, and then link them with the pre-compiled library file "UDE_f3d.lib", shown in Figure 5 and Figure 6. To

do this, the “MAKEFILE” (in ANSYS 11.x version) or “ANSYS.LRF” (ANSYS 12.x) version should be edited and the name of library file should be added to the end of it. Detailed steps can also be found in the “User Guide”.

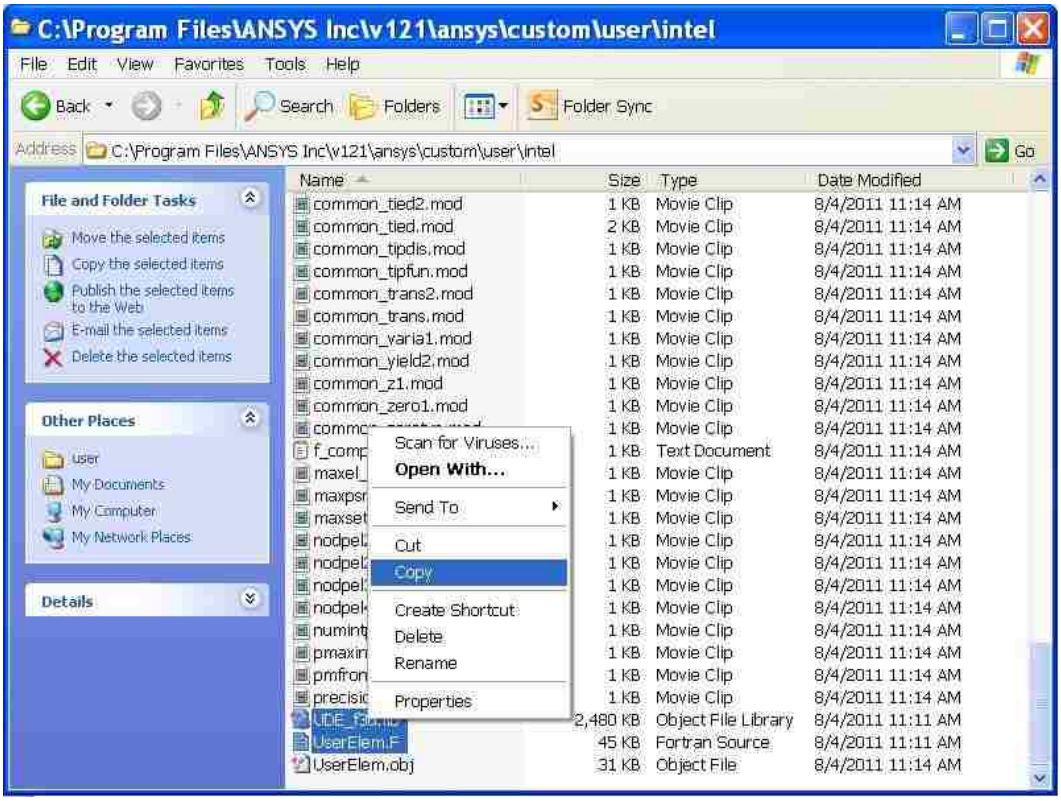

Figure 5 Copy and substitute the UDE_f3d.lib and UserElem.F from successfully compiled desktops

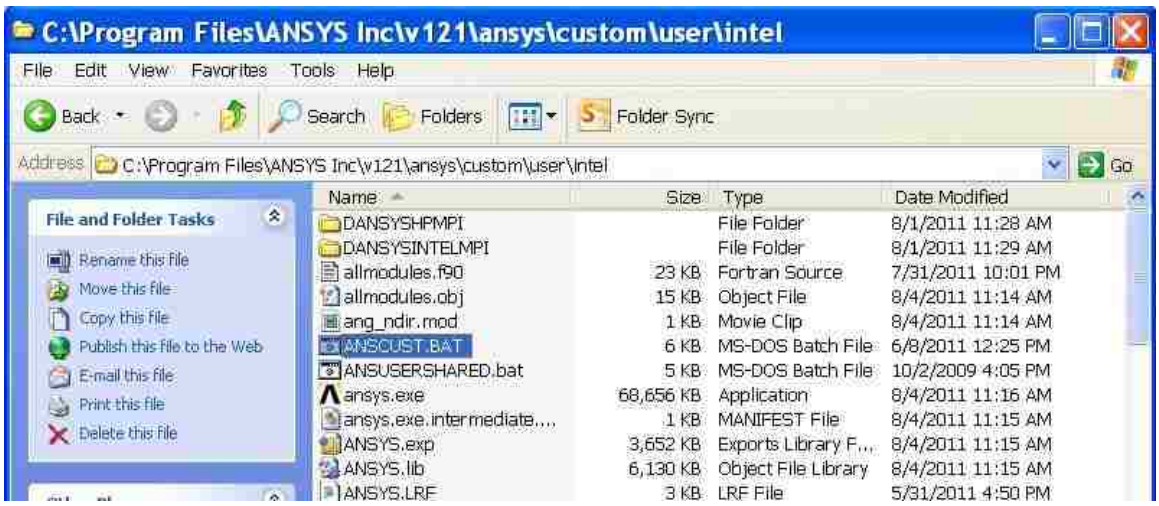

Figure 6 Use ANSYSCUST.BAT to create a User Defined “ansys.exe”

2.4 Comparison of FRAC3D and USER300

Compared with the original calculation done in FRAC3D, the new analysis process will benefit the users with integrated modeling, meshing and solving inside ANSYS framework. Figure 7 illustrates the differences between the original method of computing (Left) and the new method in ANSYS.

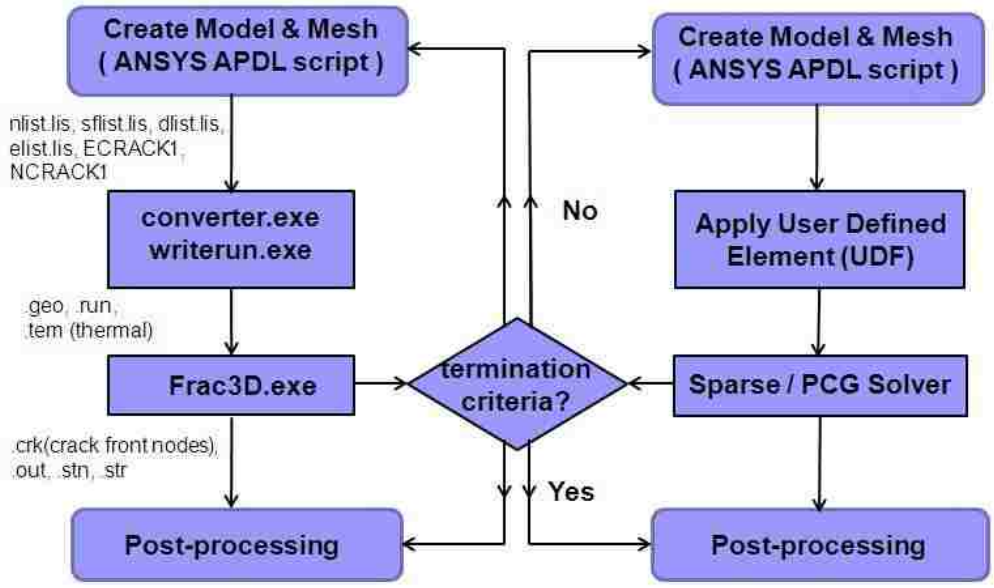

Figure 7 Comparison of the flow charts of calculation procedure

As we can notice from the above flow chart, the original way of perform the enriched finite element analysis is quite complicated, and contains many steps. Also, since the main "SOLVE" is done through a customized code "FRAC3D", researchers have to export the .nlist, .dlist, .elist, ECRACK1 and NCRACK1 files (files containing node, displacement, element, crack front element, and crack front node information) out of the ANSYS. Then, a converter.exe is needed to convert the ANSYS formatted files into FRAC3D recognized files for solving. Also, a writerun.exe file is needed to work as a "guide" so that it helps FRAC3D get some preliminary information for the crack calculation. For example, in writerun executable, the research is asked

whether it is a crack/thermal problem, and how many cracks does the model contain. The researcher is also asked to specify the crack front node and element file, as well as the model geometry file. Finally, the user is asked to define what type of finite element should be employed to mesh the crack front elements. Although this process is not hard to learn, it limits the application of the enriched finite element.

Compared to the FRAC3D process on the left part of the flow chart, the ANSYS USER 300 process on the right part is much more simplified. User can create the solid model and mesh in ANSYS, then substitute the elements attached to the crack front with enriched finite element, USER 300, and this whole process is almost finished. This is because the previous compiling work has already integrated all special features in FRAC3D into ANSYS user defined element. Thus, users can just solve the problem inside ANSYS with its Sparse or PCG solver. The whole processing time and steps has been greatly improved and is suitable for being widely used.

3 Computation

3.1 Review of Fatigue Crack Growth Propagation

Unlike the theory of brittle fracture, where the equations governing the fracture are derived from well-known laws of physics, the mathematical description defining fatigue crack growth are less precise, in which the formulation is almost based on the observations of the physical world. Lacking a firm theoretical foundation, various fatigue crack growth laws has been proposed over the last 40 years.

3.1.1 Stages of Fatigue Crack Growth

The life cycle of fatigue crack growth can are now generally categorized into three main stages, which can be represented in the following diagram, Figure 8.

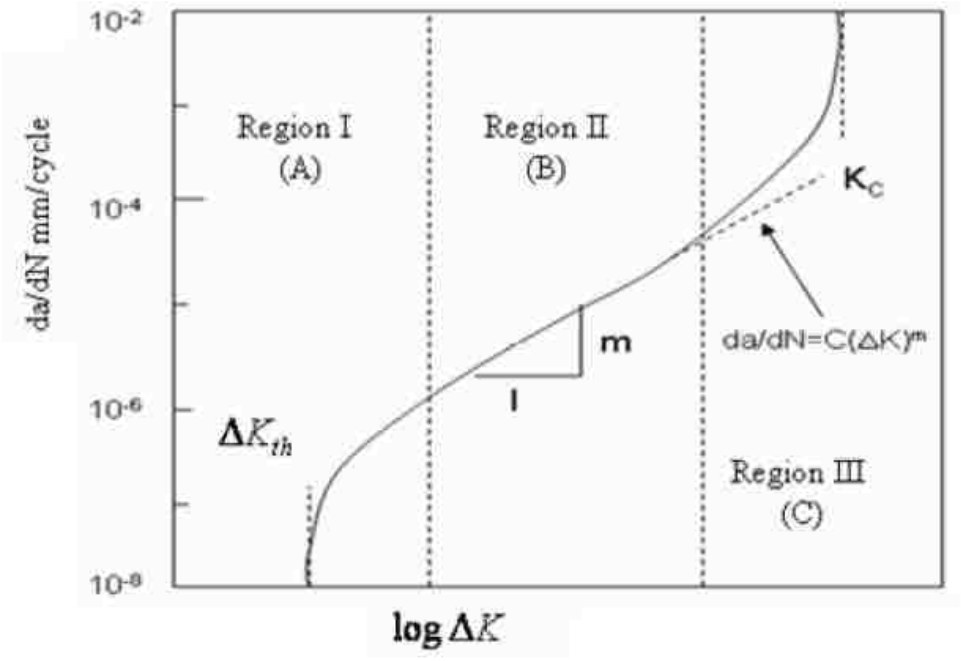

Figure 8 Stages of the Crack Propagation

Region I shows the early formation of a fatigue crack and crack growth rate. This region is largely influenced by the microstructure of the material: grain size, mean stress of the applied load, operating temperature and the environmental factors.

One significant feature of region I that is the fatigue crack should not propagate, at where the Stress Intensity Factors (SIFs) are below the so-called fatigue crack growth threshold, represented as ΔK_{th}. The value of ΔK_{th} is usually determined by experiment using the decreasing K test, described in ASTM E-647. A lot of fatigue crack propagation testing or experiment start with this stage to initiate a small micro-crack that can be used for the following stage II of the experiment.

Region II represents the intermediate crack propagation zone, in which the length of the plastic zone in front of the crack tip is long compared to the mean grain size. The stage II of crack growth in ductile materials are governed by the same mechanism: slip band motion along preferred shear planes.

There are a few observed factors that are either known to or may possibly influence fatigue crack growth [20]:

(a) During each load cycle, the fatigue crack growth occurs in discrete increments and can be expressed in the form of da/dN. As is observed in optical or electron microscope of the fatigue crack surface in many materials, striation marks are shown in the spatial period to the measure of crack growth rate, Figure 9.

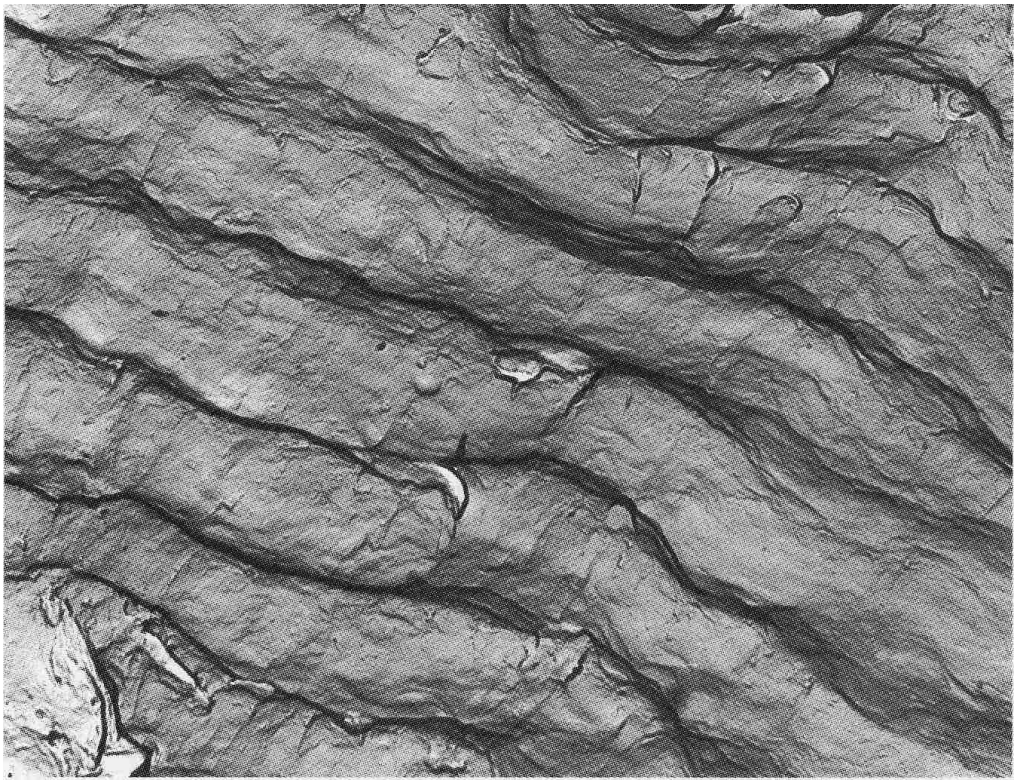

Figure 9 Fatigue Striations in Stainless Steel (Courtesy C.D. Beachem, P.E.)

(b) Crack extension corresponds to opening mode: once the initial surface crack has grown beyond initiation phase, the crack turns to be perpendicular to the applied tension. Surface toughness tends not to be a factor of interest, since there is no shear motion between shear surfaces.

(c) The crack growth rate is sensitive to the change in applied load per cycle, $\Delta\sigma$. High cycle fatigue is observed to occur only when the applied stresses are small compared to the yield stress. Also, since the single cycle crack extension is very small compared with the in-plane dimensions, the elastic stress state in the body is unaffected by the crack growth.

3.1.2 Classic Models for Fatigue Crack Propagation

(1) Paris-Erdogan Model

There are a lot of different mathematical models to characterize the crack growth phenomenon. One of the famous methods for the prediction of fatigue crack propagation is proposed by Paris and Erdogan in 1963, and is known as the Paris-Erdogan Law. The equation reflects the first application of fracture mechanics to fatigue crack, expressed by the following relation:

$$\frac{\mathrm{da}}{\mathrm{dN}} = C_p(\Delta K)^{mp} \tag{1}$$

where a is the local crack length, N is the number of cycles, *Cp* is the intercept, and mp is the slope on the log-log plot of da/dN versus ΔK and thus describes region II of the fatigue rate diagram. The Paris-Erdogan law is simple to use, and requires only the determination of two fitting parameters, so this law is commonly used as the data follows a straight line relationship.

However, the limitation of the Paris-Erdogan Law is also obvious, it only describes the stage II data (see Figure 8), which means if the data appears in the threshold (stage I) or accelerated growth (stage III), this law is inadequate to describe.

(2) Walker Model

One of the major limitations of the Paris-Erdogan Law is that it cannot account for the stress ratio. Walker (1970) improved Paris's model by including the effect of stress ratio. Walker introduced the parameter ΔK, which is an equivalent to the maximum stress intensity factor, K_{max} that causes the same crack growth rate. The expression is given below:

$$\overline{\Delta \mathrm{K}} = \frac{\Delta \mathrm{K}}{(1-\mathrm{R})^{1-\gamma \mathrm{W}}} \tag{2}$$

where,

$$K_{max} = \frac{\Delta K}{1-R} \tag{3}$$

and equation (3) becomes

$$\overline{\Delta K} = \frac{\Delta K}{(1-R)^{1-\gamma_W}} \tag{4}$$

Therefore, the Walker Law is finally represented as:

$$\frac{da}{dN} = C_w\left[\frac{\Delta K}{(1-R)^{1-\gamma_W}}\right]^{mw} \tag{5}$$

The importance of this equation is it allows a log-log plot of da/dN versus ΔK to have a single straight line regardless of the stress ratio for the data obtained. The ability to account for the stress ratio is the introduction of γ_W, and when γ_W equals one, the Walker Law is the same as the Paris-Erdogan Law. In fact, the Walker's law is a modification of the Paris's law, which takes the stress ratio effect into account.

(3) Forman Model

Though Walker law has a significant improvement to Paris law, which accounts for the stress ratio, neither of the models can take care of the instability of the crack extension, especially when the stress intensity factor approaches the critical value. Forman (1972) improved Walker's model by the introduction of a new model which is able to describe stage III of the fatigue rate curve and accounts for the stress ratio effect at the same time. Forman law is exhibited in the following relationship:

$$\frac{\mathrm{da}}{\mathrm{dN}} = \frac{C_F(\Delta \mathrm{K})^{my}}{(1-R)Kc-\Delta \mathrm{K}} = \frac{C_F(\Delta \mathrm{K})^{my}}{(1-R)(Kc-\mathrm{Kmax})} \quad (5)$$

3.1.3 System-Level Packaging Thermal Management and Optimization

The previous section 3.2 mainly describes the chip-level electronic packaging; however, a higher level of the electronic packaging would be a component or component level packaging or system level packaging. In this section, the thermal management of an electronic system will be presented, and optimize the operating temperature of its components.

Thermal management of electronic components and systems has leaded the development of advanced heat transfer techniques for the past 60 years. The advantage of better reliability, increased power, and the ever smaller size would have not been possible without the development of modern thermal management design and analysis.

The primary objective of thermal management is to prevent the electronic component from catastrophic thermal failure, the break of electronic connection, or even total loss of its electronic functionality. These failures are usually caused by thermal fracture of a mechanical support element or the separation of leads from external connections.

A second objective of thermal management is to achieve lifetime reliability of the electronic system. The control of working temperature of the system and device itself serves as the main factor to achieve this purpose. It is estimated that the failure chance of each chip, increases almost exponentially with its working temperature [21]. Thus, the temperature of critical components must be minimized, especially in a very large scale electronic system with many inside components.

3.2 3D Modeling of Interface Crack in ANSYS

3.2.1 Geometry and Load

In this part, a nice example with known theoretical solution was used to demonstrate the solution procedure for a fracture mechanics problem using the UDE in ANSYS. The model is consisted of a circular (penny-shaped) crack embedded in a BCB/silicon semi-infinite solid, Figure 10. Remote pure mechanical loading was applied on the top surface of the solid, and the bottom surface was anchored on the ground. Also, the temperature of the model cools from 200°C to 20°C with the rate of 5°C/min. The 3D finite element mesh for a quarter of the solid (1/4 symmetry was considered here) is shown in Figure 11. During the cooling of the electronic device, thermal expansion mismatch between the two different packaging materials will necessarily cause large stress between them.

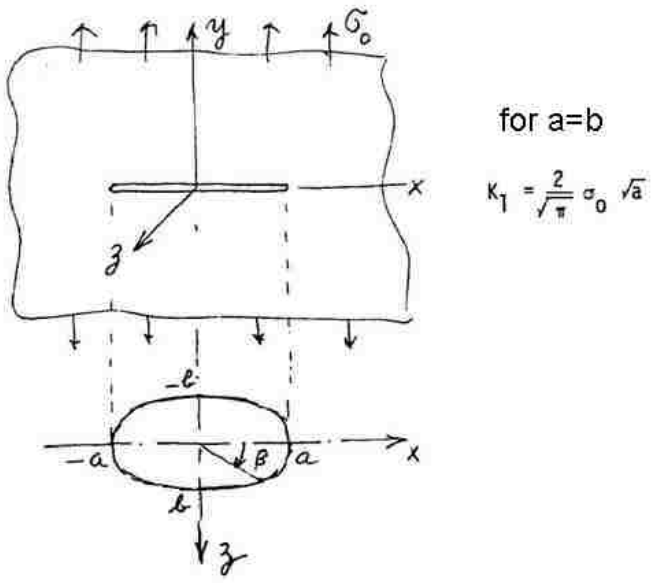

Figure 10 Circular cracks in an infinite solid as a special case of an elliptical crack

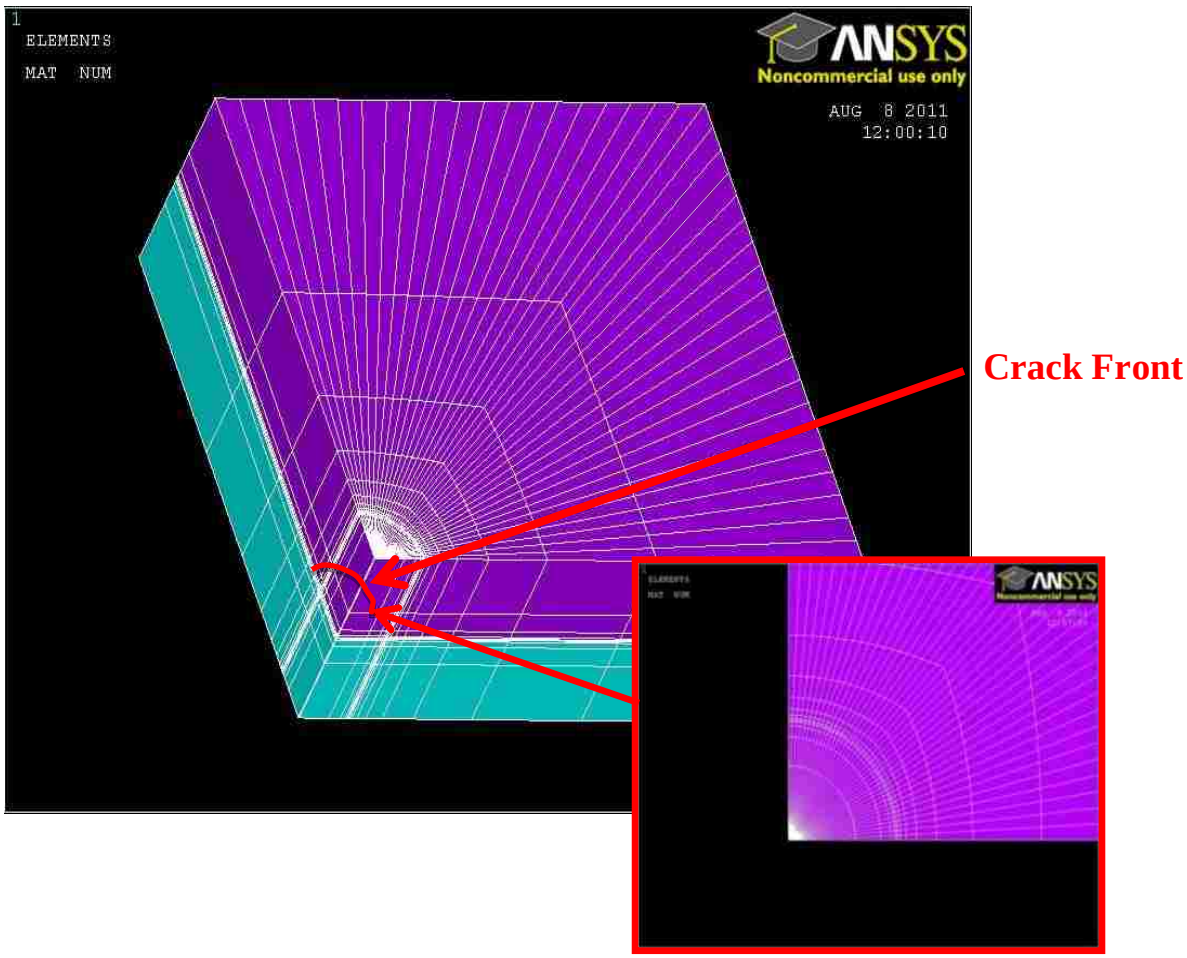

Figure 11 ¼ model of Silicon/BCB interfacial crack propagation under thermal loading

As we can notice here, the model itself is a ¼ square bulk, but contains a quarter circular crack at the corner. This causes some difficulties in attaining a fine meshing, because the radius at the tip of the corner is 0. Thus, a quarter arc with very small radius was created at the tip of the corner, instead of having infinite radius corner tip. Now, 40 nodes are evenly separated on both crack front, as well as the accessory corner tip arc, this allows a much refined meshing at the corner of this model.

3.2.2 Material Property and Fatigue Algorithm

It can be easily noticed in Table 1, the thermal expansion coefficient of the two packaging materials: Silicon and Benzocyclobutene (BCB) is of enormous difference, where the thermal expansion coefficient of BCB is almost 20 times larger than the silicon. Hence, initial crack at the interface of the bi-material packaging will eventually propagate, driven by a large stress caused by the thermal expansion mismatch.

It is also necessary to mention that, no external body forces or fields are applied to this model. The only loading of the device is the thermal stresses between the bi-material interfaces, caused by the different thermal expansion coefficient of the two materials. The temperature decrease is $\Delta T = -5°$ C/min.

Table 1: Material properties of silicon and benzocyclobutene (BCB) [8]

Material	Young's Modulus, E	Poisson's Ratio, v	Thermal Expansion, α
BCB	2.9 GPa	0.34	5.2×10^{-5}
Silicon	128.28 GPa	0.279	2.6×10^{-6}

The prediction of crack propagation relies on a formula of the Paris-Erdogan crack growth law, which is expressed by equation shown in the previous section:

$$\frac{\mathrm{da}}{\mathrm{dN}} = C_p(\Delta K)^{mp} \tag{1}$$

In order to calculate the interface crack propagation, we have to make a few assumptions first. The first crack propagation requires the calculation of strain energy release rate along the existing crack front. Then, since the both silicon and steel are isotropic materials, then parameter C and m are thus material constants. For each iteration, we define the $\Delta a_{\max}$, which is the

maximum crack front advance distance a fixed value, 0.1mm. Now, the crack propagation calculation can be carried out continuously.

After starting with an initial crack configuration, the simulation of fatigue crack propagation begins by determining the maximum ΔG value among the crack front nodes obtained. The node with this maximum ΔG is then advanced by a specified increment $\Delta a_{\max}$ as shown in Figure 12. The increment in the number of cycles, ΔN, can then be calculated directly from the difference form of eqn.(1), i.e., $\Delta N = \Delta a_{\max} \cdot \left[C(\Delta G)^m \right]^{-1}$. The Δa_i values corresponding to this value of ΔN can then be computed for each node by using the respective ΔG values in (1). This procedure is repeated, with sequential re-meshing, until a "final" crack length or number of cycles has been achieved.

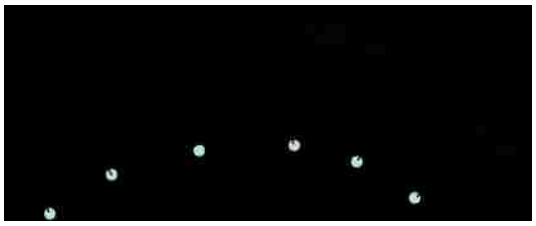

Figure 12 Advance of the crack front nodes in crack growth algorithm method.

3.2.3 Apply Enriched UDE

Having meshed model and the loading condition defined, the next step is substituting the elements along the crack front with UDEs. By simply change the element type from "SOLID95" to the "USER300", all the elements attached to the crack front are specified as the UDEs Figure 13. Some necessary parameters are input through a series of newly created graphic multi-dialogs Figure 14.

After this step, the creation of solid model and meshing is done, the elements attached to the crack front is also substituted with the Enriched Finite Element, USER300. Now, we can just set up the ANSYS solver, and ready for the computation. In this model, we selected the PCG solver provided by ANSYS, because PCG solver provides numerical iteration, and is usually more stable and more accurate as opposed to the SPARSE direct solver, which is based on direct elimination of equations [22].

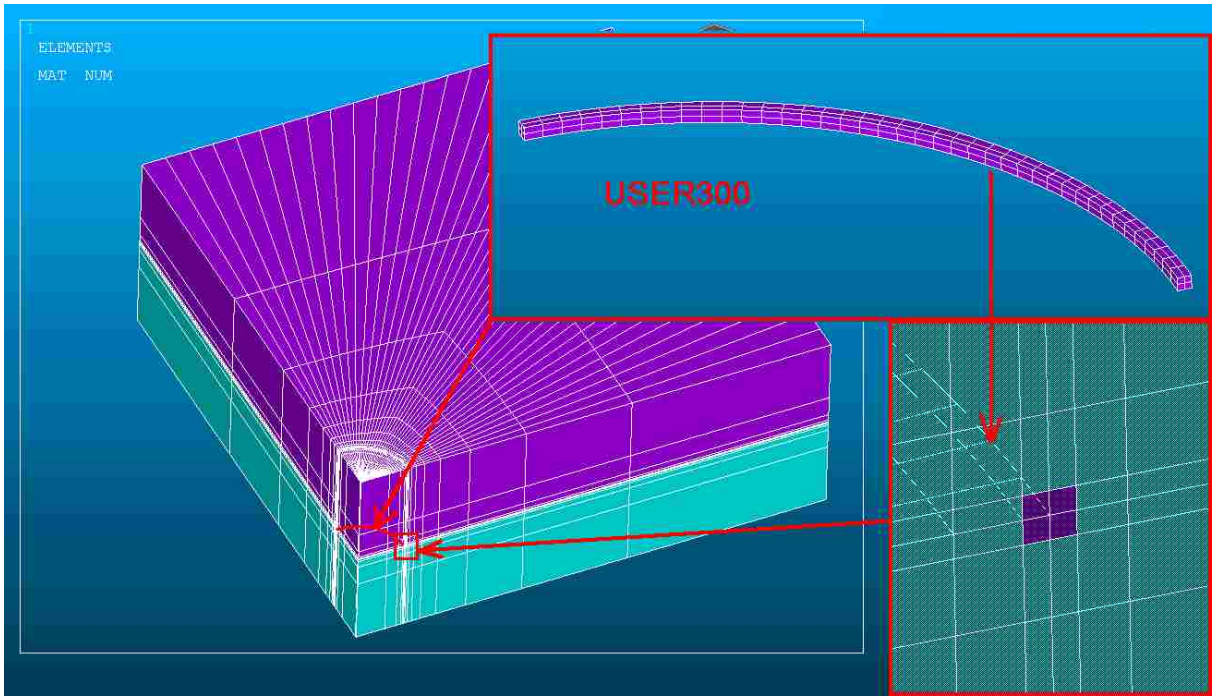

Figure 13 User Defined Elements (USER300) along the crack front

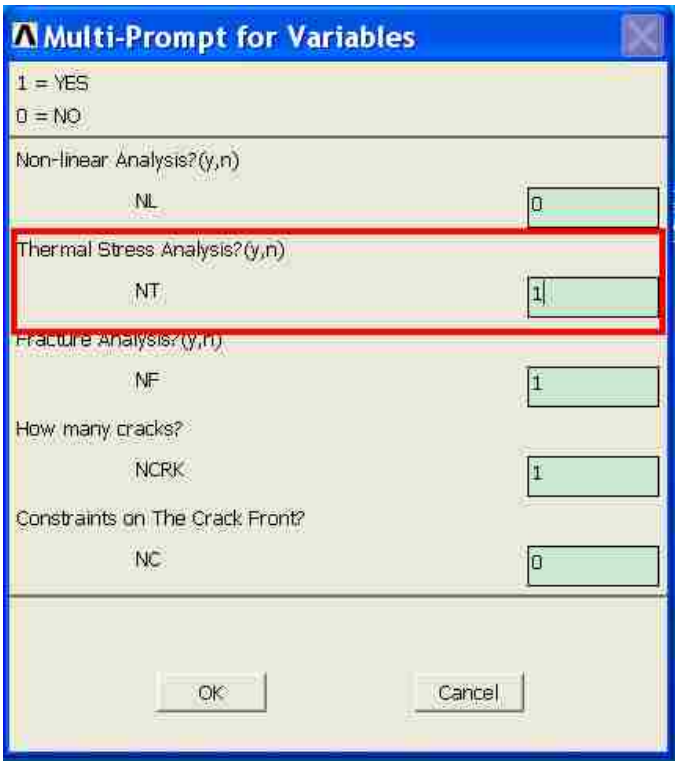

Figure 14 Multi-dialog indicating the basic information of the computing

3.3 3D Modeling of System-Level Package

3.3.1 Processing and Flow Chart

The follow study will use ANSYS Workbench as a platform, and employ ANSYS IcePak as main module for the thermal flow management design and simulation. As is indicated in the following work flow (Figure 15) of the Workbench, a solid model of personal electronic system was first created in the software Pro-Engineer, and the model file is saved in the IGES or STEP format so that it could be used in ANSYS without losing any geometric information. Here, the solid model is saved in the STEP file, and is then imported into the Workbench and become an ANSYS recognized model.

After that, IcePak module was dragged into the framework, and the solid model is now linked into the IcePak for future analysis. The goal is to optimize this electronic system and manage its thermal flow, and decrease the core temperature the critical electronic device.

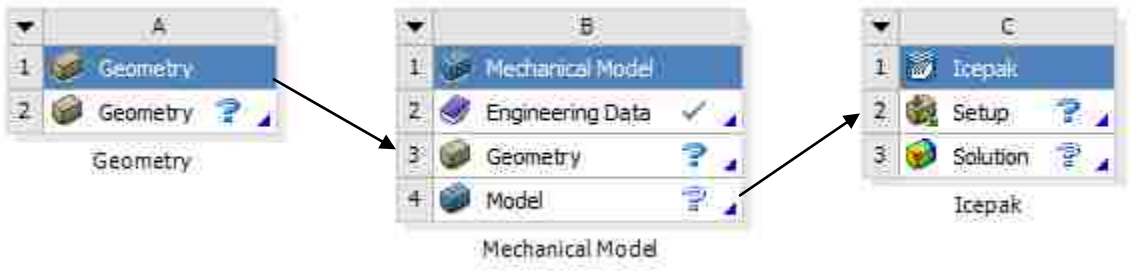

Figure 15 Flow chart of conducting simulation in ANSYS Workbench

3.3.2 Configuration of the System

(1) Solid Model and Meshing

The first configuration of this electronic system is originated from an older version of a commercial available personal desktop, which contains a PCB as its motherboard, a CPU chip

package with the heat dissipation assembly, two hard disk drives (HDD), two memory (RAM), one DVD-ROM, one 3.5” floppy disk drive (FDD), a power supply unit (PSU); 80mm system cooling fan and a GPU package. Tabulated parameters of the electronic system can be found in Table 2, where dimension, quantity, material and power of each electronic device are included.

Device	Quantity	Dimension (mm)	Material	Power (W)
PCB	1	250×250	Silicon	n/a
CPU chip	1	50×50	Silicon	10
HDD	2	140×100×20	Metal	5
DVD-ROM	1	180×130×40	n/a	3.59
FDD	1	130×140×30	n/a	n/a
PSU	1	145×135×100	Metal	n/a
Fan	1	∅80	n/a	n/a
GPU	1	150×70	n/a	7
RAM	2	130×30	Silicon	0.5

Table 2

In order to simplify the simulation, some components with minor influence on the thermal analysis was ignored and thus not included in the solid model. For example, all electric resistances and capacities emit heat in almost each component, but since they are relatively small and are not critical to the whole system, they are not included in the simulation. Other devices like the motor of the system fan, though it dissipates heat and is of quite high temperature when works, but it is not taken into account because the fan itself is the main component.

Some components however, though they do not usually emit heat into the system during the service, the volume of these devices are large enough to change the flow direction and properties inside the electronic system, so they are considered here as well. One example of these components is the floppy disk drive: it has low power and does not radiate heat at working, but it

has a volume of 130×140×30, so it is still considered as a critical component in the simulation. Figure 16 shows the solid model of the system configuration #2 created in the Pro-Engineer.

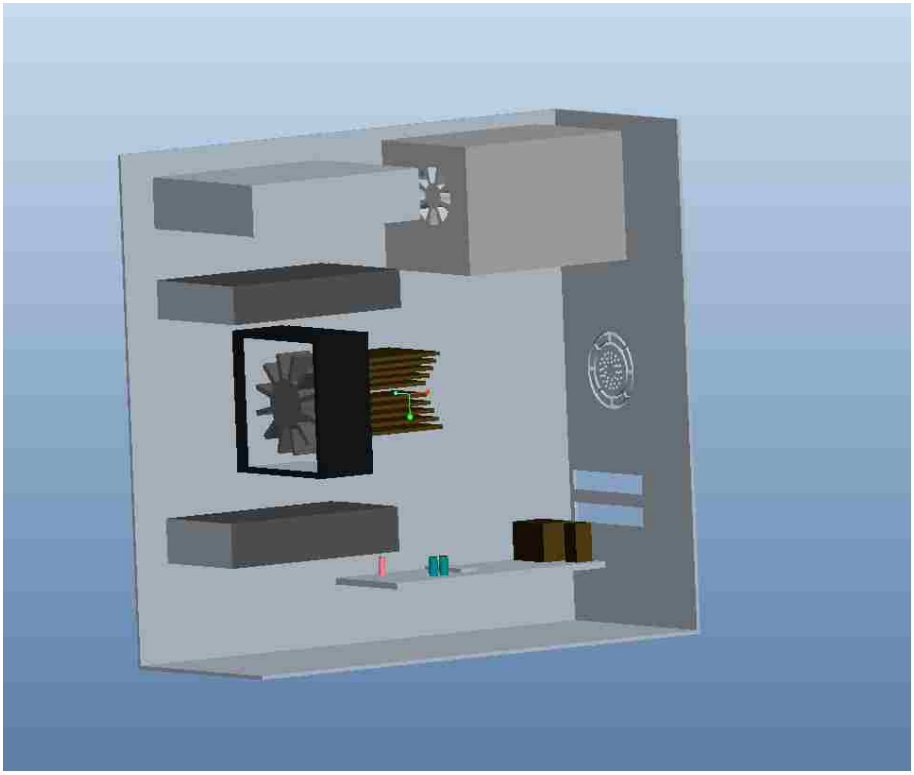

Figure 16 Solid model of the electronic system in Pro Engineer

With this solid model ready, the next step is to import it into the IcePak for further analysis. As is shown in Figure 17 (a), the solid model is imported into the IcePak through Workbench.

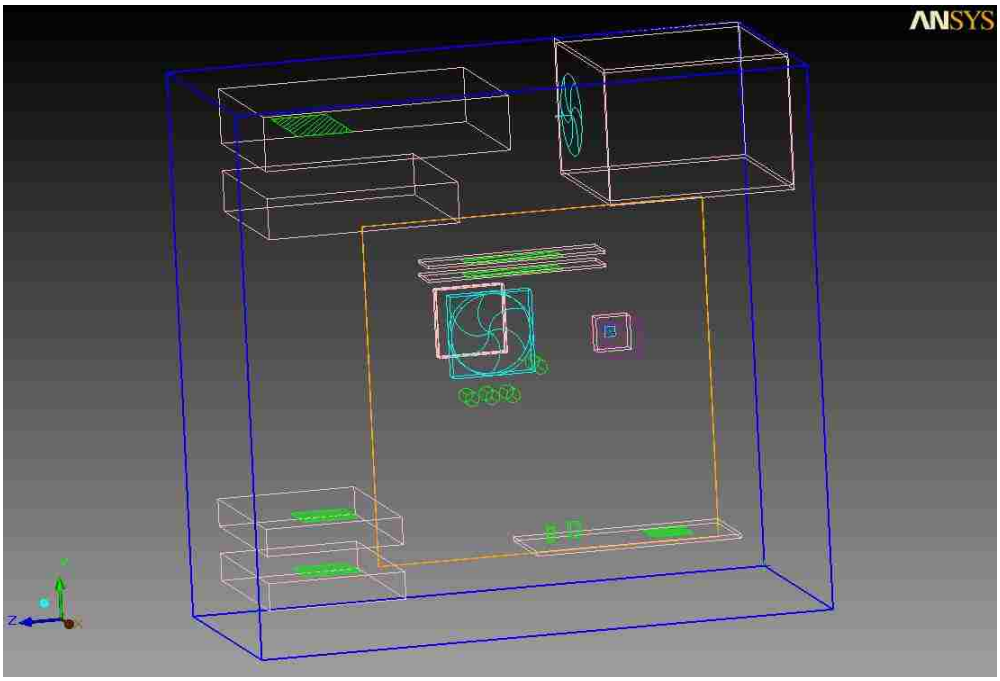

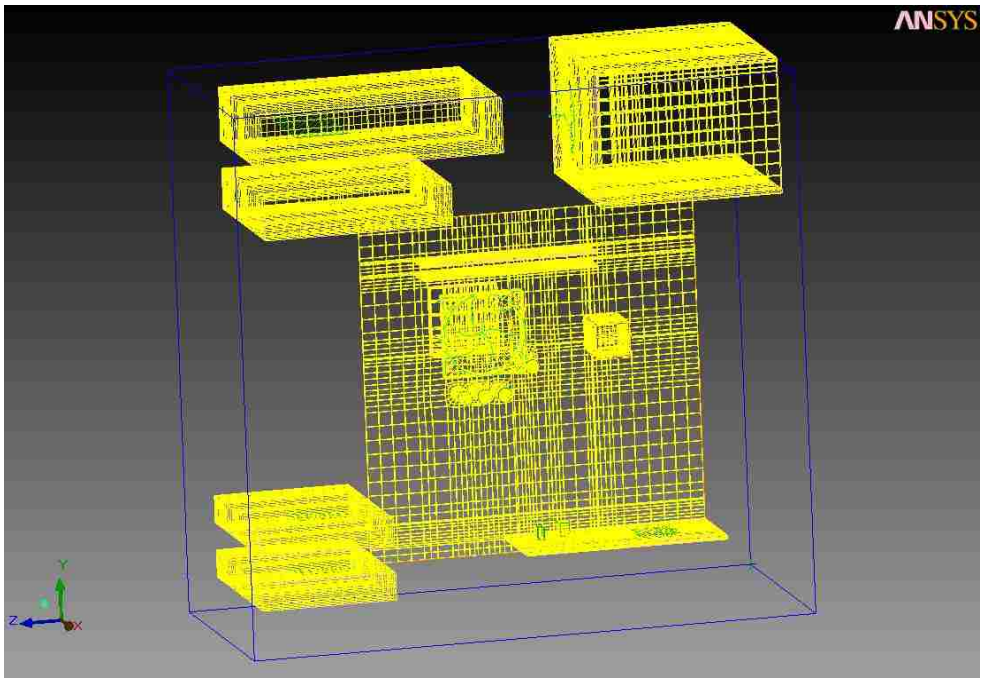

Figure 17 (a) Solid model of the electronic system #1 in IcePak (b) Meshing of the Electronic system #1

It is noticed in Figure 17 (b), however, after the solid model was transferred into the IcePak, all solid parts was transferred into lines and surfaces. This is because in IcePak, the imported

models are simplified into electronic geometries, which means the solid models are redefined specifically for electronic application.

The model is then meshed in the IcePak. Here, we used Multi-Level Meshing (MLM) in IcePak, which provide a means to improve the mesh resolution and optimizing the mesh count of a model [23]. It is easily noticed that the meshing of critical components are denser than the other parts. The maxim meshing density ratio is 5:1. For this model there are 413,523 elements and 436,553 nodes, where 255,637 of the elements are improved meshing elements. The Multi-Level Meshing allows us to improve the mesh resolution of critical components and have a smooth transition to coarser meshes. Hence, it reduces the overall mesh count and significantly reduces computational run time while enhances the accuracy of the simulation.

3.3.3 Optimized Configuration of the System

The second configuration of this electric system is based on the simulation results of the first one, where the fan is repositioned as a system fan, instead of mounting onto the CPU. An aluminum heat sink is mounted on the CPU instead. This is because in the first configuration, heat dissipation is not very effective, the flow inside system become mixed turbulent due to the inappropriate direction of the system fan. Also, the temperature of CPU chip was over 80°C, which is very close to the critical CPU temperature of 90°C ~100°C of the most commercial used CPU. Detailed analyze could be found in the following section 4, where simulation results of thermal and mechanical solutions will be discussed.

The optimized configuration is shown in the Figure 18, where MLM is still implemented to reduce the run time while maintain the computational accuracy. For this setting, 426,005 elements and 449,679 nodes are presentd, where 278,556 are refined elements for the critical parts, shown in Figure 18.

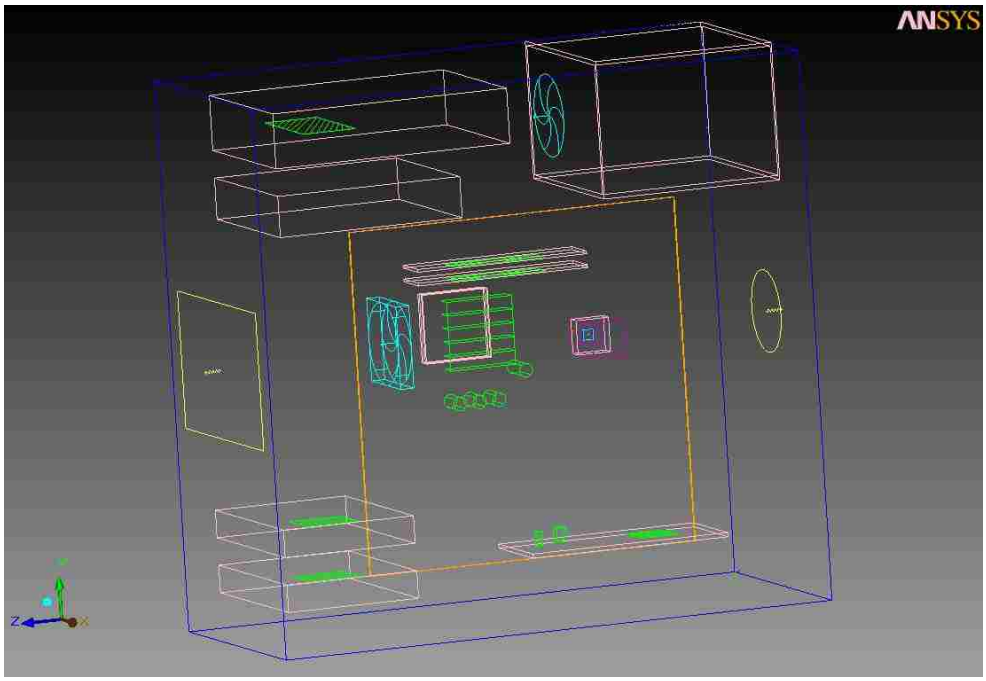

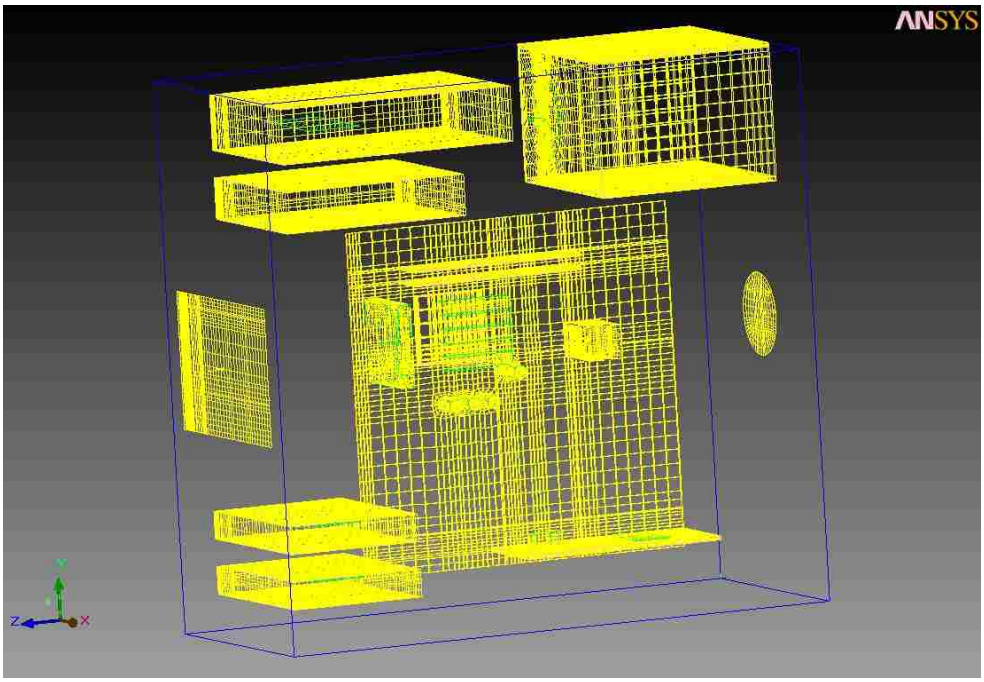

Figure 18 (a) Solid model of the electronic system #2 (b) Meshing of the electronic system #2

4 Result and Conclusion

4.1 Crack Problem Solution

By running the model with ANSYS PCG solver, the time consumed for computing has been greatly decreased. It used to take over 5~6 hours to finish the 80 cycle crack propagation in FRAC3D, but with the ANSYS PCG solver and USER 300 enriched element, this processing time of the same model become 1.5 hour. The final crack propagation is depicted in the sequence of curves shown in Figure 19. It is noticed that at the first several steps, both ends of the crack propagated larger distance than the middle part, which is also consistent with the first stress intensity factor K1 shown in Figure 20. The magnitude of K1 is largest at the both ends of the crack, which indicates there is the largest stress intensity. Thus, the both ends of the crack will propagate faster than the rest. This is also observed in the experimental interface crack growth behavior for corner cracks subjected to thermal cycling, as well as the previous result from FRAC3D.

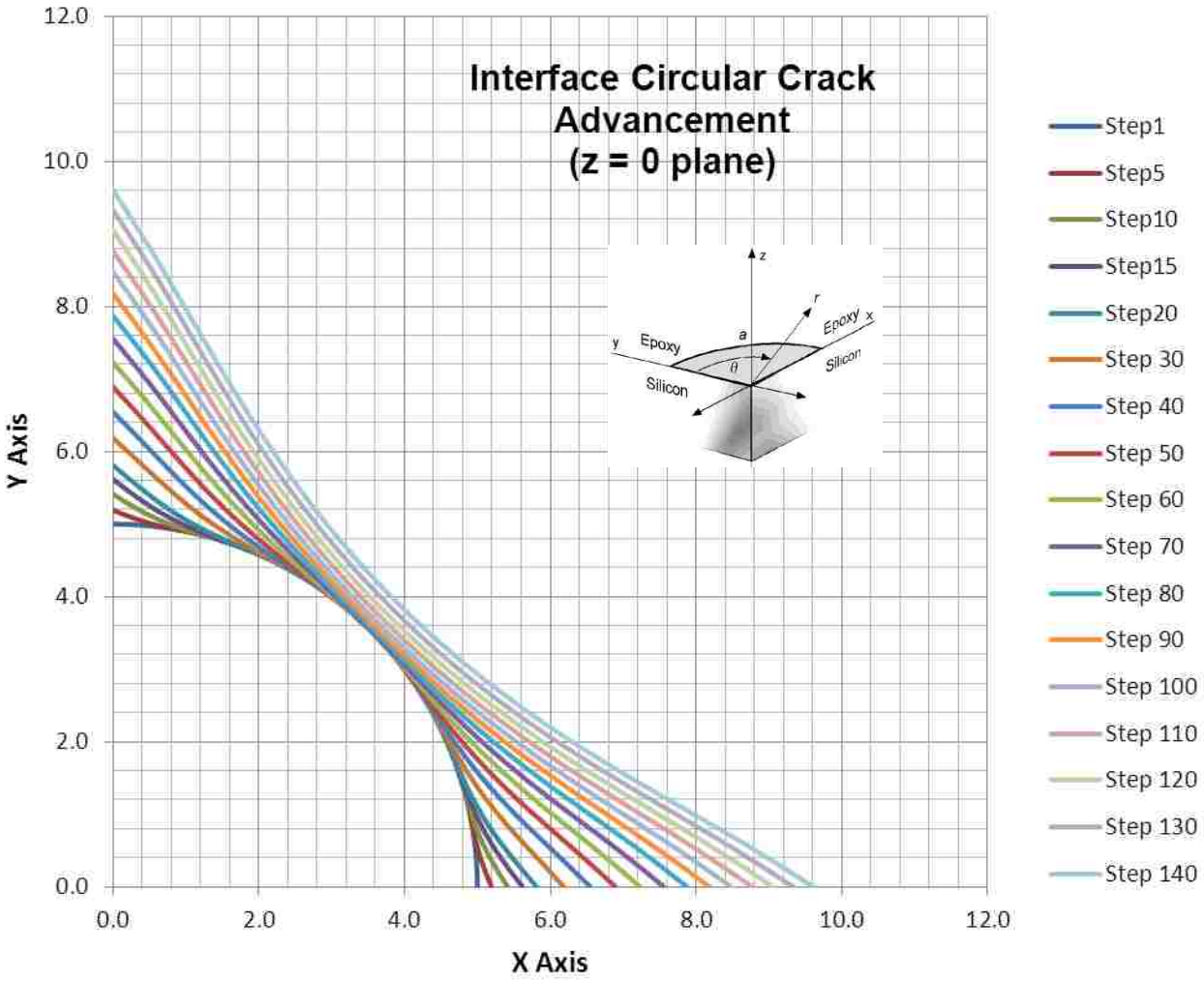

Figure 19 Interfacial crack propagation of the bi-material under thermal loading

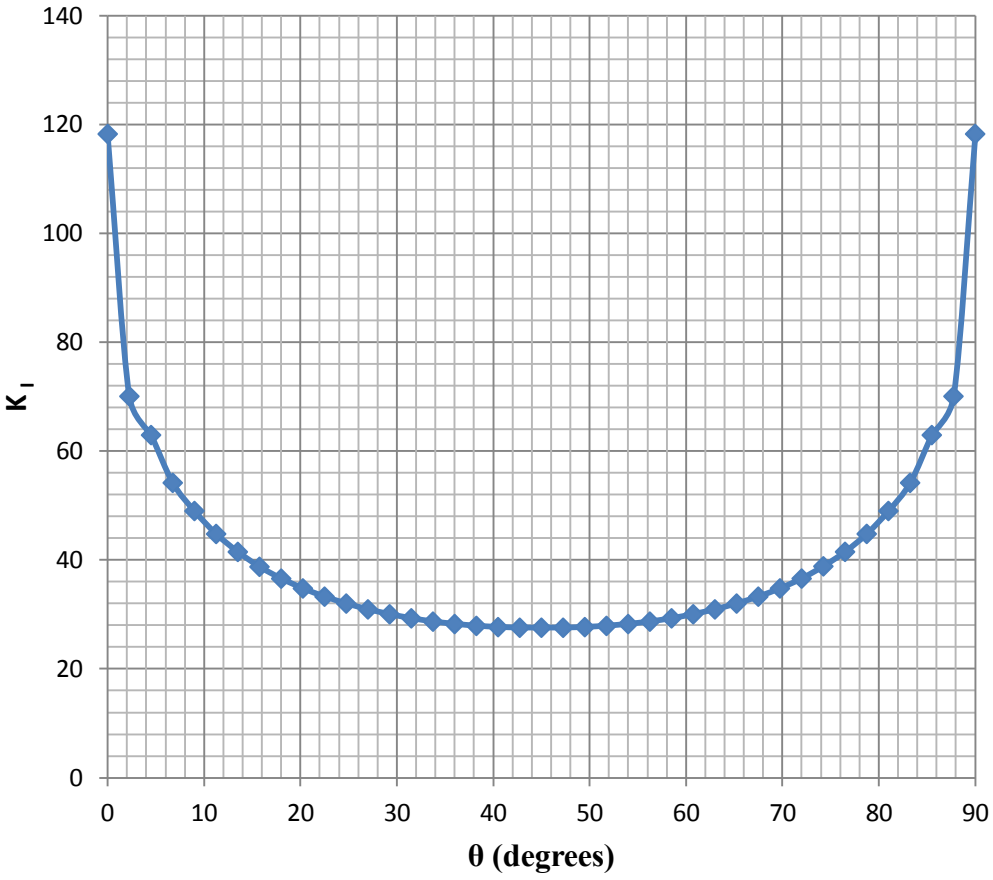

Figure 20 First stress intensity factor, K I along the crack front

4.2 Thermal Management Solution

4.2.1 Case #1 Fan mount on chip

Heat transfer status of the electronic system is shown in Figure 21: the highest temperature is 80.34°C, which occurs at the center of CPU. However, since we are more interested in the temperature of critical component, CPU, a detailed temperature contour for each device is shown in the Figure 22. Here, the average temperature of the whole PCB mother board is 65°C, while the 80.34°C core temperature of CPU is close to the 90°C~100°C critical value. Also, since the manufacturer recommends the working temperature of CPU 20°C under its critical value, 80.34°C is still considered an overheating of the device.

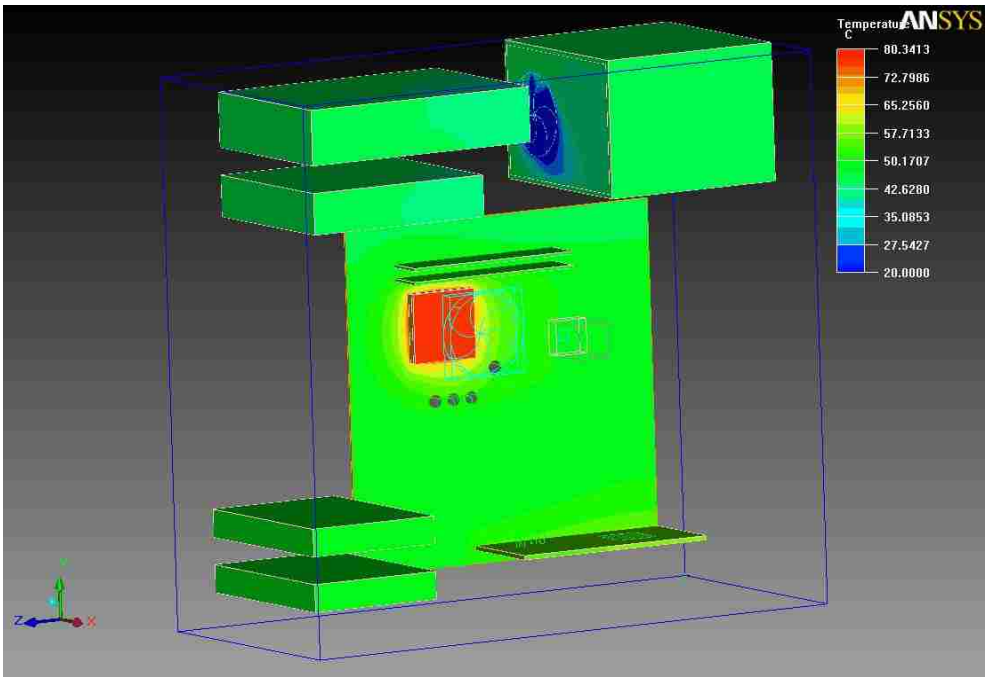

Figure 21 Temperature distribution of the electronic system #1

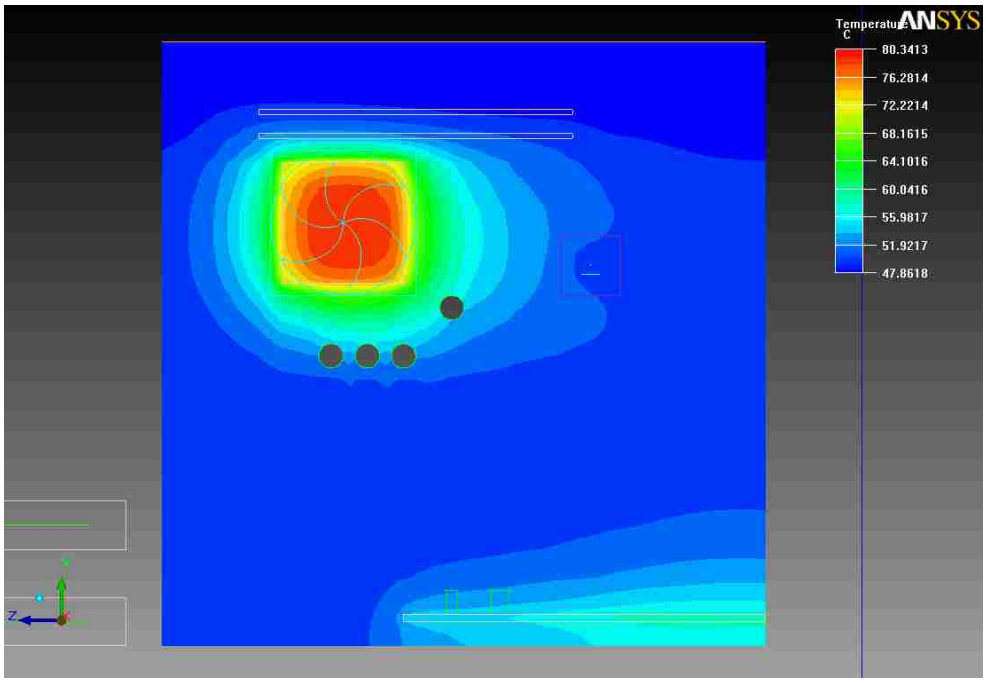

Figure 22 Temperature distribution of the PCB board in system #1

The cause of heat transfer results can be explained by the flow status of the inside system. As we can see in Figure 23, the highest speed of the in-house flow rate is 2.225 m/s, and the lowest

speed is 0 m/s, which indicates at some area of the system, no flow exchange happens there. The median airflow speed is 1.113 m/s.

Another interesting phenomenon we have found in the airflow of Figure 23 is that the flow exhibits as turbulent flow at both top and bottom of the CPU assembly. This kind of circulation is also not favorable, because it indicates the high-temperature-airflow is concentrated around the CPU chip, and is not transferred outside of the system.

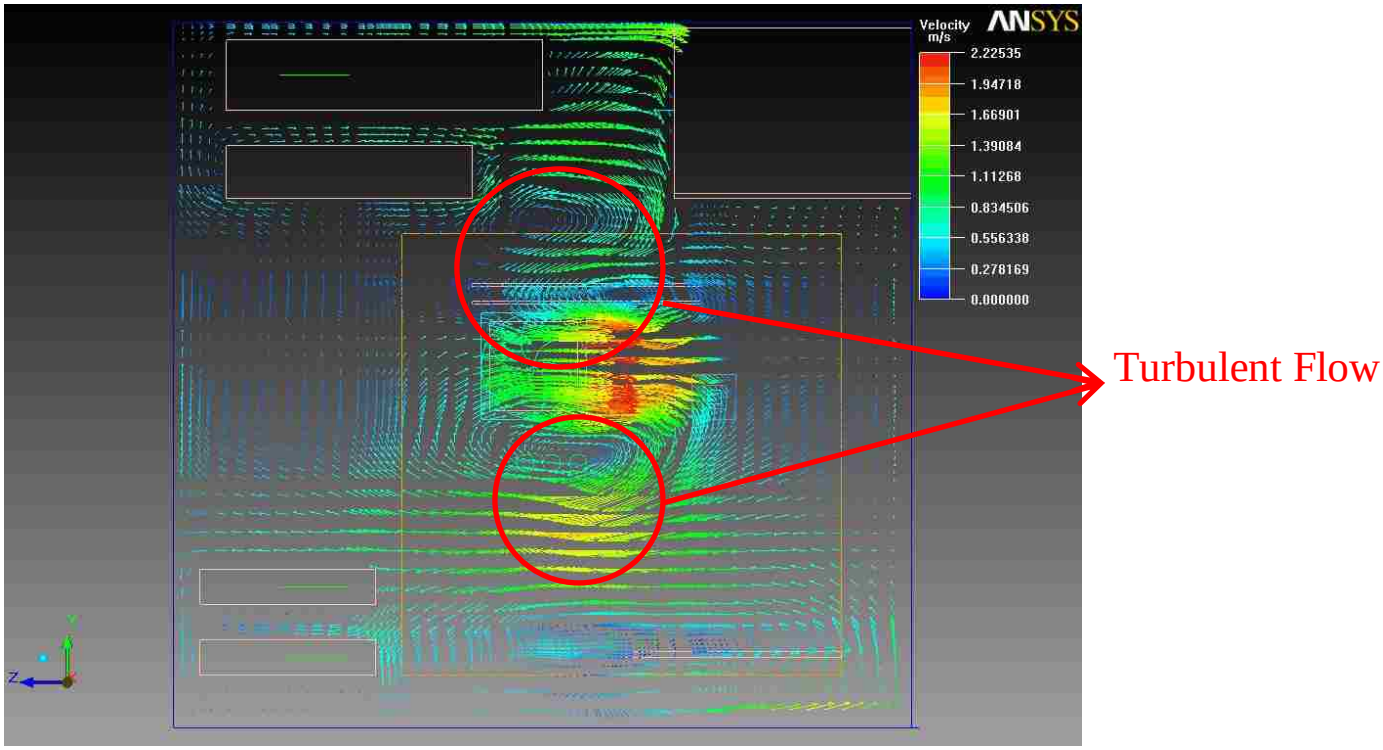

Figure 23 Airflow speed contour in the system configuration #1

4.2.2 Case #2 Fan mount on body with heat sink on chip

Since the cooling effect of system configuration 1 is not desirable, a second system configuration is presented. This setting is also the current model of this desktop. It should also be mentioned here that almost all parameters (Material, Dimension, Power, and Quantity) of the electronic

devices have not been changed. Their relative location to the housing was not changed either. Thus, the solid model of the first system can still be used.

One significant difference between the two systems lies at the heat dissipation assembly of the CPU. It is shown in the previous section, Figure 18 that the system fan on the new configuration was reversed and mounted perpendicular to the CPU chip, while an additional heat sink was installed on the chip. Hence, the CPU chip is cooled through this heat sink, by directly conduct heat to the sink. Instead of blowing airflow perpendicular to the CPU ship, the fan now blows air parallel to it, in the X-Y plane direction. Finally, two openings were created both at the front and rear panel of the system cabin, which are used as the inlet and outlet of the airflow. They can be easily noticed in the below Figure 24, where the front inlet is a rectangular shaped window, and the rear outlet is a circular window.

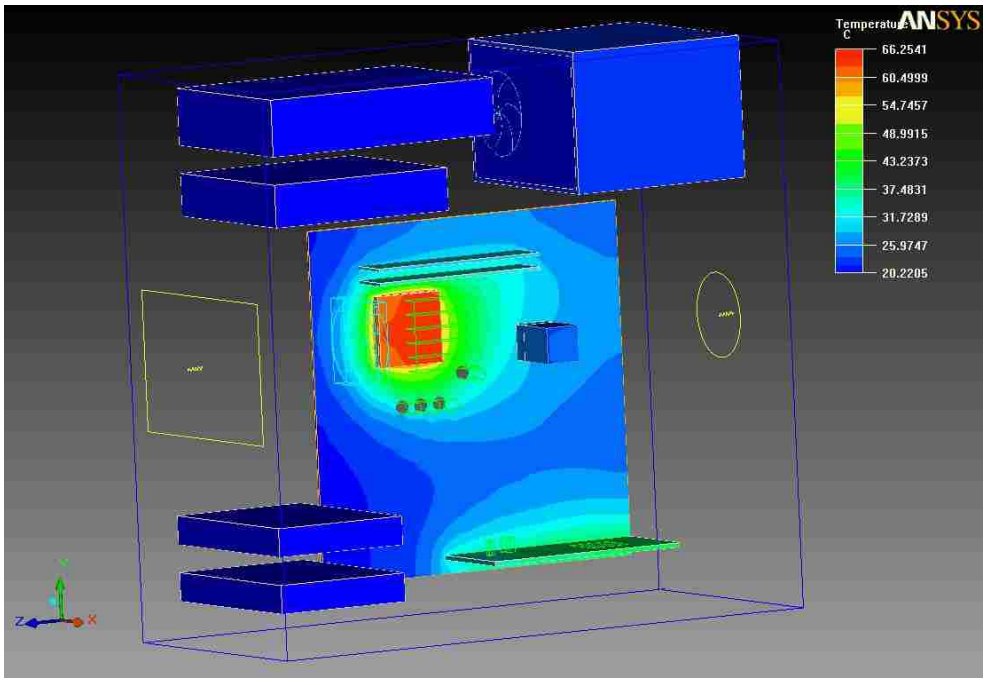

Figure 24 Temperature distribution in the system #1

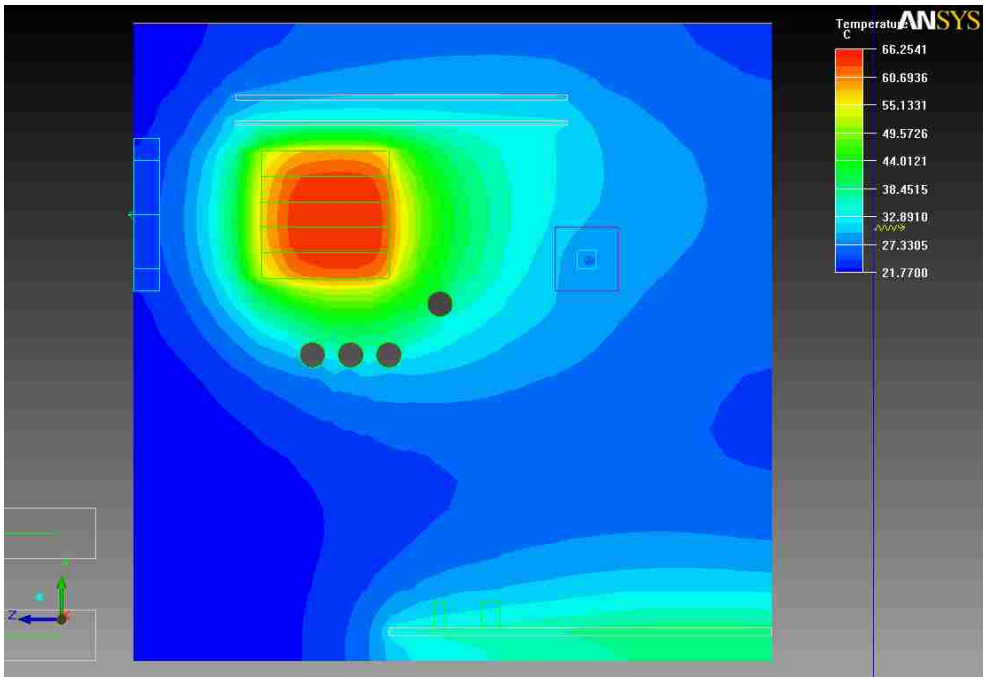

Figure 25 Temperature distribution of the PCB board in system #2

The effect of the new settings on heat dissipation was remarkable. It can be easily noticed in Figure 25 that the peak temperature at the center of CPU chip decreased from the previous 80.34°C to 66.25°C, which is 17.5% cooler than that in the first system configuration. In addition, the average temperature of the system turned out to be 44°C. Compared to the previous system average temperature of 65°C, the current temperature is 32.3% lower.

In this system configuration, the fan is used as a central cooling device. It helps bring away the heated airflow on the heat sink. A second but very important function of the vertical mounted fan is it helps improve the ventilation of the electronic system. Again, we can easily tell this from the Figure 26, the speed contour of in-house airflow. Here, the top speed of the airflow occurs at the system outlet, which is 3.044 m/s, while the median speed was 1.522 m/s. Compared to that in the first configuration, the top speed increased 36.8% and the median increased 36.7%. Higher speed of airflow indicates a larger flow rate through the system and thus better ventilation.

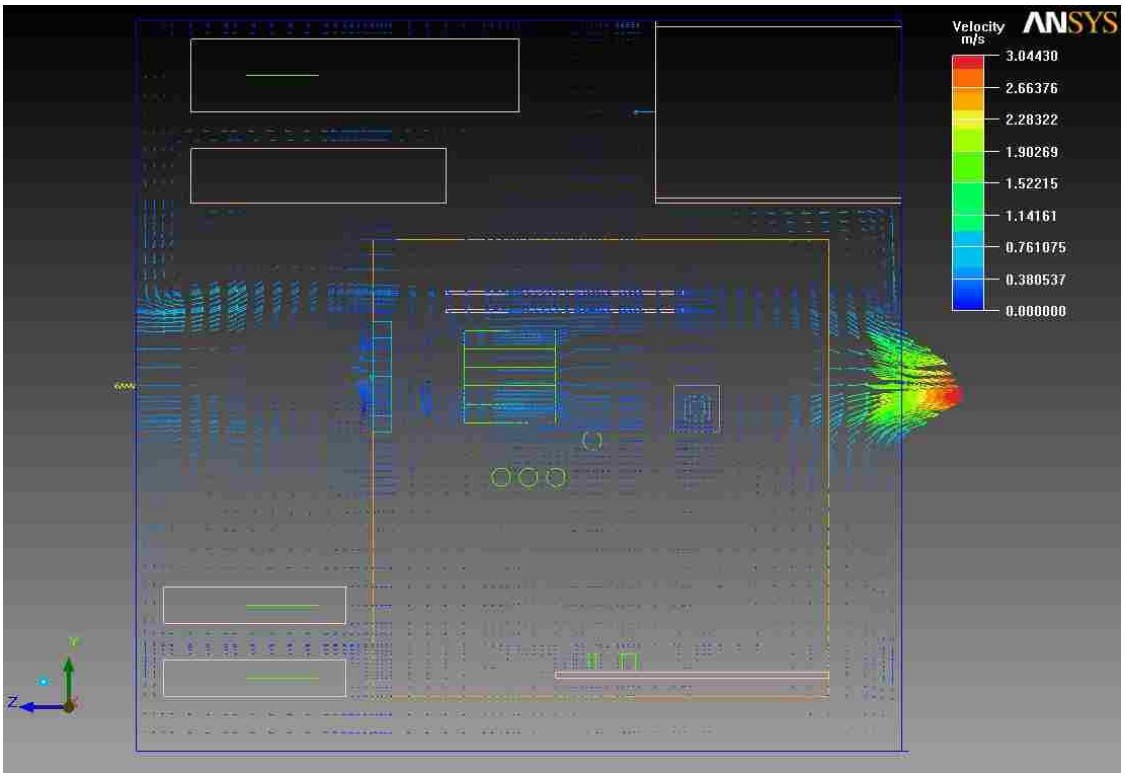

Figure 26 Airflow speed contour of the system configuration #2

Beside the improved circulation of the airflow, for the status of the airflow, Figure 23 indicates a totally different airflow in the second setting. Here, the airflow inside the system cabin is steady, laminar flow, which is significantly different from the unsteady, turbulent flow in the first configuration.

In conclusion, the aluminum sink helped the heat on chip assembly to conduct; a vertical mounted system fan increased the flow rate in ambient to the aluminum sink and bring away the heated airflow; two big openings of inlet and outlet helped guide the airflow inside the system and increased the circulation. In all, the new configuration of this electronic system was verified to be more efficient than the horizontally mounted fan in the first configuration.

4.3 Conclusion

In this study, enriched finite element was seamlessly incorporated to the customizable "USER 300" element, by using the ANSYS User Defined Features. Three additional degrees of freedom, the stress intensity factor K1, K2 and K3 enabled the calculation of asymptotic fracture mechanics. The prediction of 3D interface fatigue crack growth was performed using the results of stress intensity factors of the crack front nodes, together with the classic crack growth theorem.

The result showed that new method of simulation was very efficient, and it is especially true for the iterating the fatigue problem by ANSYS PCG solver. Average computing time for the current interface fracture propagation model was 70% less than using FRAC3D. The result showed that the final shape of the corner crack after 80 cycle of propagation matches with the shape of experimental result quite well. This also matches with the previous conclusion from Alex Herr [16], that the final shape of the crack front tends to be a straight line.

Compared to traditional method of performing the calculation with FRAC3D, the UDF allows modeling, meshing, simulation and post processing as a package inside the commercial available FEA software ANSYS. This helps a broader application of the Enriched Finite Element Method in both academia and industry.

Finally, new features in the ANSYS WorkBench and IcePak allow users to simulate large scale, multi-physics problems with the integration of framework. It also provide with better connection for the FEA software with other 3D modeling software, which makes the simulation of complicated geometry, with assemblies and different electronic packages become possible. With the workbench and IcePak, thermal and mechanical problems in electronic packaging are "easier" than before.

5 Future Work

3D interface crack propagation was done in this study by using the macro in ANSYS APDL. For each crack propagation step, macro is executed again and takes the result from previous step as a new input. Although compared to the previous method of using different executables and running them from one to another, this method is a great progression and save 70% of computing time, there is still some inconvenience. For each iteration, all solid model and meshing is regenerated again, which is not an optimized processing. This is especially true when the solid model is of complicated geometry, for example: the flip chip assembly or BGA with solder balls, because for the crack propagation, there is no need to have the whole solid model regenerate again and mesh again, only nodes at the crack front needs to be repositioned. One method of doing this is creating a series of different sub models with pre-crack, which are of different geometries to suit with complicated geometry of the real solid model. For example, the researcher creates three different sub-models: brick-shaped rectangular model, triangular shaped model and tetrahedral shaped model, and all these three models with different shape contain a pre-crack in them. Once the user wants to create a crack in their real solid model, he/she can just import the sub-model and put them at specific area where crack usually initiates.

Secondly, the USER 300 enriched finite element allows user calculate stress intensity factors, and made the calculation of asymptotic crack tip fracture mechanics possible. However, in order to use this customized element, users are first required to recompile a customized ANSYS executable with the FORTRAN compiler. Necessary preparation work has to be done before successfully use the USER 300 element. An alternative way of doing this is to create an element library and make it as a macro for the ANSYS. It is just like customized material library, which contains special material properties or non-linear stress-strain relation.

Finally, the ANSYS WorkBench and IcePak are introduced here to demonstrate its ability of doing thermal and mechanical analysis specific for electronic packaging problems. They have better compatibility with other 3D solid modeling software compared to classic ANSYS APDL. However, the final objective is to use the results from IcePak or WorkBench as a new input, and incorporate it with the analysis for crack problem. An issue with this process is that the current version of WorkBench has only limited user customizable features that allows user to write their own subroutines. IcePak, however, have no definable features at all. So how to make the system-level thermal/mechanical results from IcePak benefit the crack tip fracture mechanics with thermal loading become a very interesting problem. Figure 26 provides a logic flowchart that how ANSYS IcePak and ANSYS APDL can work together. They both import their data (geometry, mesh, setup and solution) into the WorkBench, and perform desired calculation inside the ANSYS WorkBench Figure 27.

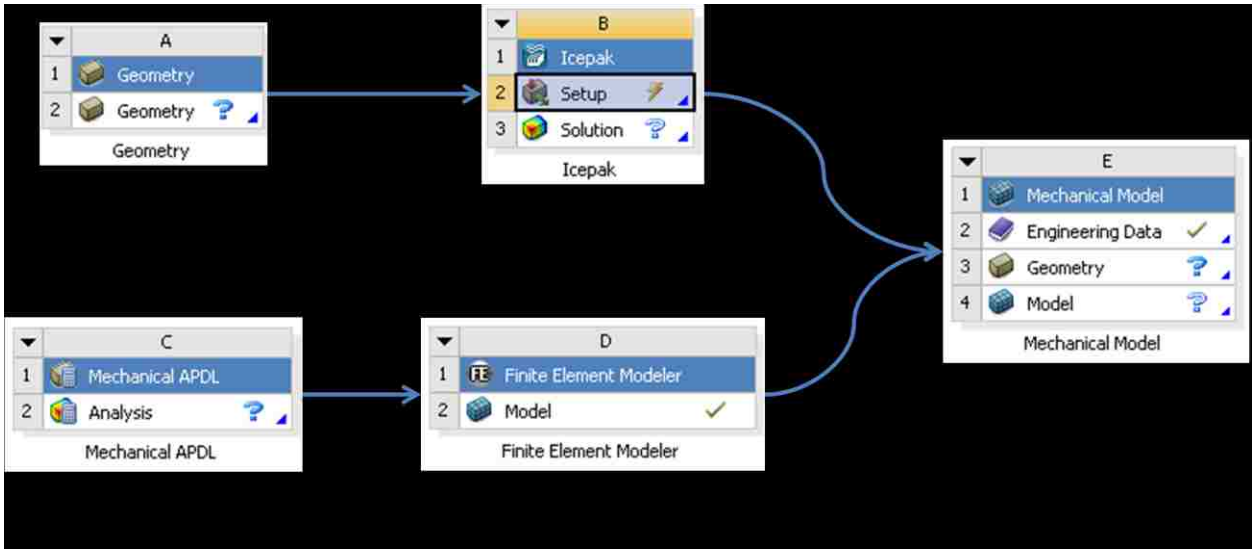

Figure 27 Flow chart for the feasibility of joint work of IcePak and APDL

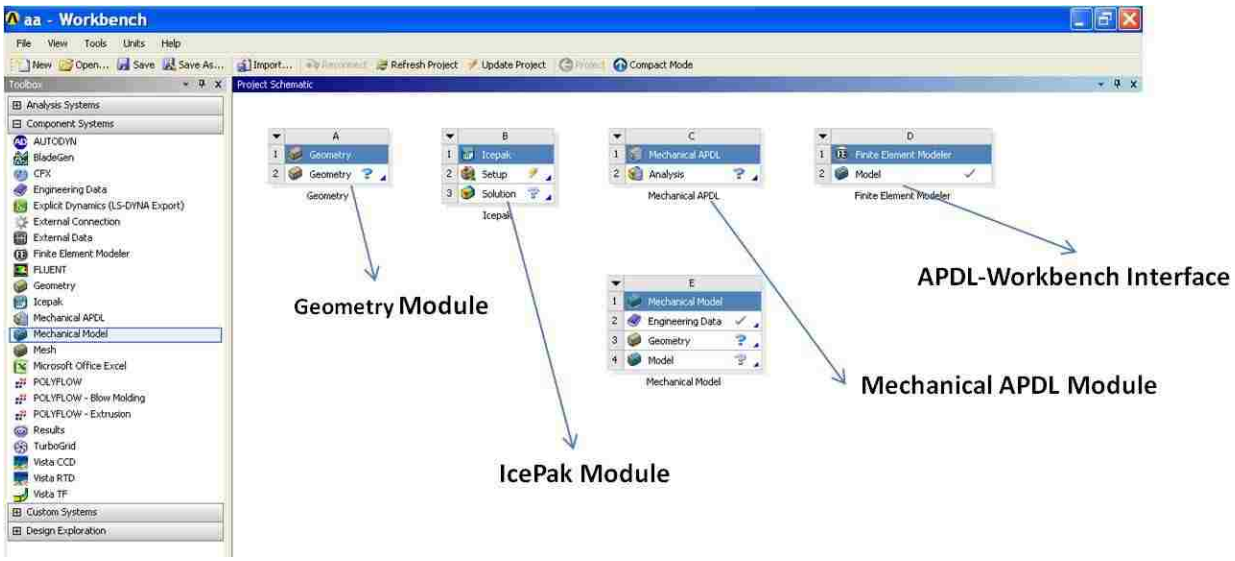

Figure 28 Different modules for the multi-physics simulation in WorkBench

6 List of Abbreviations and Symbols

PTH: Plate Through Hole

SMT: Surface Mount Technology

BGA: Ball Grid Array

PCB: Printed Circuit Board

SIFs: Stress Intensity Factors, K

FEA: Finite Element Analysis

FT: Fracture Toughness

UPFs: User Programmable Features

DOF: Degree of Freedom

3D: Three Dimensional; Three Dimensions

MEMS: Microelectromechanical System

Reference

[1] t. f. e. Wikipedia, "Fracture Mechanics," 2012. [Online]. Available: http://en.wikipedia.org/wiki/Fracture_mechanics.

[2] S. K. Kang, "Lead (Pb)-Free Solders for Electronic Packaging," *Journal of Electronic Materials,* vol. 23, pp. 701-707, 1994.

[3] B. Su, Y. Lee and M. L. Dunn, "Die Cracking at Solder (In60-Pb40) Joints on Brittle (GaAs) Chips: Fracture Correlation Using Critical Bimaterial Interface Corner Stress Intensities," *Journal of Electronic Packaging,* vol. 125, pp. 369 - 337, 2003.

[4] S.-B. Lee, I. Kim and T.-S. Park, "Fatigue and fracture assessment for reliability in electronics packaging," *Internal Journal of Fracture Mechanics,* vol. 150, pp. 91-104, 2008.

[5] R. J. Sanford, "Elasticity of Singular Stress Fields," in *Fracture Mechanics,* 2003, p. 56~57.

[6] P. Widas, "Introduction to Finite Element Analysis," Virginia Techn Material Science and Engineering, 8 4 1997. [Online]. Available: http://www.sv.vt.edu/classes/MSE2094_NoteBook/97ClassProj/num/widas/history.html.

[7] Wikipedia, "Finite element method," Wikipedia the free encyclopedia, [Online]. Available: http://en.wikipedia.org/wiki/Finite_element_method.

[8] D. Roylance, "Finite Element Analysis," Massachusetts Institute of Technology, Cambridge, 2001.

[9] A. Inc, "ANSYS WOrkbench User's Guide," SAS IP, Inc., Cannonsburg, 2010.

[10] T. Seelig, D. Gross and K. Pothmann, "Numerical Simulation of a mixed-mode dynamic fracture experiment," International Journal of Fracture, Darmstadt, 1999.

[11] h. D. Espinosa and B. Peng, "A New Methodology to Investigate Fracture Toughness of Freestanding MEMS and Advanced Materials in Thin Film Form," *Journal of Microelectromechanical Systems,* vol. 14, pp. 153-159, 2005.

[12] C. Mareau, V. Favier, B. Weber, A. Galtier and M. Berveiller, "Micromechanical modeling of the interctions between the microstructure and the dissipative deformation mechanisms in steels under cyclic loading," *International Journal of Plasticity,* pp. 106-120, 2010.

[13] H. B. Fan, P. Chung, M. Yuen and P. Chan, "An energy-based failure criterion for

delamination initiation in electronic packaging," *J. Adhesion Sci. Technol.,* vol. 19, pp. 1375-1386, 2005.

[14] J. Snodgrass, D. Pantelidis, M. Jenkins, J. Bravman and R. Dauskardt, "Subcritical Debonding of Polymer/Silica Interfaces Under Monotonic and Cyclic Loading," *ActaMaterilia,* vol. 50, pp. pp.2395-2411, 2002.

[15] R. Khandelwal and J. C. Kishen, "The use of conservative intergral in bi-material interface crack problems subjected to thermal loads," *International Journal of Solids and Structures,* vol. 45, pp. 2976-2992, 2008.

[16] H. N. A.F. Herr, "Numerical Simulation 3-D Mixed-mode Crack Propagation on Bi-material Interfaces," *11th Telecommunication Conference.*

[17] H. N. A.O. Ayhan, "FRAC3D-Finite Element Based Software for 3-D and Generalized Plane Strain Fracture Analysis (2nd Revision)," 1999.

[18] A. I. Southpointe, "Guide to ANSYS User Programmable Features," SAS IP, Inc, Canonsburg, 2004.

[19] Y. Chen, X. Liu, S. Murat and F. N. Herman, "User-Defined Enriched Crack-Tip Elements for ANSYS," Lehigh University Mechanical Engineering and Mechanics, Bethlehem, 2011.

[20] R. Sanford, in *Principles of Fracture Mechanics*, Upper Saddle River, NJ, Pearson Education, Inc., 2003, pp. 291-294.

[21] B. William, in *Advanced Electronic Packaging*, New York, IEEE Press, 1998, pp. 178-179.

[22] A. Inc, "Types of Solvers," ANSYS 11.0 Documentation, [Online]. Available: http://www.kxcad.net/ansys/ANSYS/ansyshelp/Hlp_G_BAS3_4.html.

[23] A. Inc, "ANSYS IcePak Tutorials," SAP IP, Inc, Cannonsburg, 2010.

Vita

Yi Chen was born on November, 1987 in Shanghai, China. In 2006, Yi was admitted into Tongji University, School of Aerospace Engineering and Applied Mechanics, and studied Aircraft Manufacturing. During his study, Yi was awarded Dean's List at Tongji and the National Scholarship from the Ministry of Education of China. Yi has been working in a composite research group at Tongji, and studied natural fiber reinforced composites for future aircraft material.

After Yi graduated from Tongji in 2010, he came to Lehigh University, and studied in the department of Mechanical Engineering and Mechanics. Since then, Yi has been worked with Dr. Herman F. Nied and focused on the research of fracture mechanics and fatigue crack propagation in semiconductor packaging.

While doing his graduate study at Lehigh, Yi is also working as an engineering analyst at Stanley Vidmar in Allentown, where he is responsible for the product design and modification. He deals with lots of 3D modeling for sheet metal products and changes the bill of material and routing of these products in SAP system.